DESIGN OF AN AUTO CHANGE MECHANISM AND INTELLIGENT GRIPPER FOR THE SPACE STATION (RESEARCH GRANT NO. NAG 5-922)

GODDARD
IN-18-CR
217711
55 P

FINAL REPORT

BY

DIPAK P. NAIK

PRINCIPAL INVESTIGATOR: PROF. PAUL H. DEHOFF

(NASA-CR-185367) DESIGN OF AN AUTO CHANGE MECHANISM AND INTELLIGENT GRIPPER FOR THE SPACE STATION Final Report (North Carolina Univ.) 55 p CSCL 22B H2/18 N89-25268 Unclas 0217711

MECHANICAL ENGINEERING AND ENGINEERING SCIENCE DEPARTMENT
UNIVERSITY OF NORTH CAROLINA AT CHARLOTTE
N.C. 28223

(1988 - 1989)

ABSTRACT

Robot gripping of objects in space is inherently demanding and dangerous and nowhere is this more clearly reflected than in the design of the robot gripper. An object which escapes the gripper in a micro g environment is launched not dropped. To prevent this the gripper must have sensors and signal processing to determine that the object is properly grasped, eg grip points and gripping forces and, if not, to provide information to the robot to enable closed loop corrections to be made. This report describes the sensors and sensor strategies employed in the NASA/GSFC Split-Rail Parallel Gripper. Objectives and requirements are given followed by the design of the sensor suite, sensor fusion techniques and supporting algorithms.

CONTENTS

+++

LIST OF FIGURES

NOMENCLATURE

a	: Larger Side of Cross Section of Gripper Finger
b	: Smaller Side of Cross Section of Gripper Finger
d	: Center to Center Distance Between Two Strain Gauges
[C]	: Calibration matrix
dx	: Translational Displacement in X Direction
E	: Young's Modulus
E_r	: Error Vector
F_x	: Grip Force
F_{xy}	: Grip Force with Δ_y offset
F_{xz}	: Grip Force with Δ_z offset
G	: Shear Modulus
GF	: Gauge Factor
T_r	: Transformation Matrix
V_1	: Input Voltage to Bridge 1, Volts (Finger 1)
V_2	: Input Voltage to Bridge 2, Volts (Finger 1)
V_3	: Input Voltage to Bridge 3, Volts (Finger 1)
V_4	: Input Voltage to Bridge 4, Volts (Finger 1)
V_5	: Input Voltage to Bridge 5, Volts (Finger 2)
V_6	: Input Voltage to Bridge 6, Volts (Finger 2)
V_7	: Input Voltage to Bridge 7, Volts (Finger 2)
V_8	: Input Voltage to Bridge 8, Volts (Finger 2)
V_9	: Input Voltage to Potentiometer, Volts
Z	: Section Modulus

GREEK ALPHABETS

Δ_{e1}	: Output of Quarter Bridge 1, Volts (Finger 1)
Δ_{e2}	: Output of Quarter Bridge 2, Volts (Finger 1)
Δ_{e3}	: Output of Quarter Bridge 3, Volts (Finger 1)
Δ_{e4}	: Output of Quarter Bridge 4, Volts (Finger 1)
Δ_{e1}	: Output of Quarter Bridge 1, Volts (Finger 2)
Δ_{e6}	: Output of Quarter Bridge 2, Volts (Finger 2)
Δ_{e7}	: Output of Quarter Bridge 3, Volts (Finger 2)
Δ_{e8}	: Output of Quarter Bridge 4, Volts (Finger 2)
Δ_{e9}	: Output of potentiometer, Volts
μ	: Poisson's Ratio
γ	: Shear Strain
Δ_x	: Offset in X Direction
Δ_{y1}	: Y Offset on Finger 1
Δ_{y1opt}	: Desired Y Offset on Finger 1

$\Delta y2$	: Y Offset on Finger 2
$\Delta y2opt$	: Desired Y Offset on Finger 2
$\Delta z1$	: Z Offset on Finger 1
$\Delta z1opt$	: Desired Z Offset on Finger 1
$\Delta z2$	: Z Offset on Finger 2
$\Delta z2opt$	: Desired Z Offset on Finger 2
$\Delta xerr$	: Translational Error in X Direction
$\Delta yerr$	: Translational Error in Y Direction
$\Delta zerr$	: Translational Error in Z Direction
$\Delta \theta err$	: Rotational Error In Pitch
$\Delta \phi err$	: Rotational Error In Roll
$\Delta \psi err$	: Rotational Error In Yaw

+++

DESIGN OF AN AUTO CHANGE MECHANISM AND INTELLIGENT GRIPPER FOR THE SPACE STATION (RESEARCH GRANT NO. NAG 5-922)

INTRODUCTION

Robot gripping of objects in a micro g environment is inherently dangerous and demanding and this is clearly reflected in the design of the robot gripper. First, an object which the gripper is grasping is necessarily attached to something (Fig. 1) to prevent it from drifting away. Thus it cannot shift its position while it is being grasped and this in turn means that the robot and gripper must do the compliance. Second, an object which escapes the gripper is launched not dropped. Third, because the environment is space, the gripper and sensor system must be very reliable (simple) as repairs are most inconvenient.

The gripper mechanism used is the NASA/GSFC Split-Rail Parallel Gripper. This report describes our approach to instrumenting this mechanism and giving it the intelligence necessary to accomplish the requirements (sometimes conflicting) described above. The sensor system is described as are the governing equations, electronics and algorithms. Likely error modes are discussed as is the signal processing necessary to make the proper corrections. Sensor fusion techniques are presented to make use of all available existing sensory data and still keep the system simple.

LITERATURE REVIEW

Over the last nine years the state of art in robotic force/torque technology has been developed to a high degree in research laboratories such as Draper Labs, JPL, SRI, MIT and elsewhere [1- 30]. The interest of providing in some cases a robot arm with an active adaptable compliant wrist has been largely emphasized[2, 4, 19, 24]. The main component of such a wrist is a several degree of freedom force sensor. The literature [1, 2, 3, 4, 5, 6, 18, 20, 23] commonly describes sensors based upon strain gauges.

At last count there were over a dozen different transducer designs which resolve, either directly or indirectly, the forces and torques acting on the robot hand. As research tools, these sensors have relied on the host computer to calculate forces and torques from transducer readings. In addition, the host computer has been responsible for a number of associated functions such as calibrations, sensor biasing etc. Unfortunately, such systems have not found much use outside of the laboratory since their application requires considerable effort on the part of the user. Although many of the necessary tools have been developed, they have yet to be embodied in one coherent user-friendly package. This report is the result of a study to delineate those features which can be implemented on a processor dedicated to force, position and orientation sensing.

THE GRIPPER

Fig. 2 shows the schematic diagram of the parallel jaw gripper designed for our application and relies on distributed contact for a secure grasp. This gripper operates on well known rack and pinion principle, the rack being coupled to the fingers and having a common pinion which is being actuated by a d.c. motor. The racks which protrude out at either ends of the gripper during a definite portion of an operating cycle are enveloped by a protective casing. The surface of the jaw are curved with cross shaped grooves which match similar projections on object surface (Fig. 3). The gripper fingers are designed in such a way that small deflections are permissible in jaw. The design of force sensing jaws requires a compromise between elasticity and structural stiffness to avoid extensive deflections reducing the positional accuracy. The forces and their offsets are measured indirectly by four strain gauges on each jaw. The sensor environment of the gripper is minimal. The gripper maximum throw is 7 inches and its effective grip force is 100 pounds. The gripper motions are controlled by microprocessor exchanging data with the central robot controller such as position, grasp force, sensor data etc.

SENSOR SYSTEM

As teleoperation fundamentally requires static grasp, the sensor system should be able to sense magnitudes and locations of grip force accurately so that the object shown in Fig. 2 fits snugly into the corresponding recesses in jaws. Sensor system for this application must satisfy following conditions,

1. High accuracy and resolution
2. Compact size and light weight
3. Robust and Reliable
4. High sensitivity and short response time

Transducers used for measuring the six component vector describing the errors in gripper position and orientation with respect to that of the object to be grasped has to fulfil following requirements:

1. Strain range:m 0 - 1550 μ inch/inch

2. Transverse sensitivity : negligible
3. Accuracy of the measuring system: Force: +-0.25 lbs
   Torque: +-0.25 in-lbs
4. Resolution of the system: 0.5 lbs
5. Life: Load cycles 10^7 for long duration of time
6. Temperature range: -100^o to 400^o F
7. Measuring technique: Fast data logging and processing

The sensor system of the gripper to satisfy the above requirements is composed of four strain gauges on each finger as shown in Fig. 4(a). Our primary object being to accurately control magnitude of grip force F_x (Fig. 5) and its corresponding offsets Δ_y and Δ_z which locate the point of action of grip force. The sensor system presented contains four pairs of strain gauges that can sense the magnitudes and locations of grip force using an algorithm to be discussed later. Since it is difficult to predict which finger either of the two would touch the object first, both the fingers are instrumented with four strain gauges each. The gripper throw is measured through a potentiometer.

In order to vary the position of gripper to accurately align itself to grasp the object the various drives of robot joints should be controlled systematically in response to the signals coming from various transducers. The procedure to do this is elaborated as follows.

WHEATSTONE BRIDGE

Strain gauges A, B, C and D form separately quarter of a bridge as shown in Fig. 4(b). The output of the Wheatstone bridges 1 and 2 for strain gauge A and B is proportional to the bending moments M_a and M_b at gauge locations A and B. The relation between F_{xy}, M_a, M_b and d, the center to center distance between the gauges A and B is as follows,

$$F_{xy} * d = M_a - M_b$$

Bridge 1 output Δ_{e1} for gauge A now can be expressed as

$$\Delta_{e1} = F_{xy} * C_1 * d_1 / (E * Z) \qquad .....(1)$$

Where,

$$C_1 = V_1 \frac{R_1 * R_3}{(R_1 + R_2) * (R_3 + R_4)} * GF \qquad [31]$$

and

GF : Gauge Factor of Strain Gauge A
V_1 : Input Voltage to Half Bridge Circuit 1

d : Center to Center Distance Between Two Strain Gauges
d_1 : Distance Between Force F_{xy} and Strain Gauge A
E : Young's Modulus
Z : Section Modulus
F_{xy}: Grip Force with Δ_y offset
Δ_{e1}: Output of Half Bridge Circuit

Similarly output of bridge 2 for strain gauge B is as follows,

$$\Delta_{e2} = F_{xy} * C_2 * d_2 /(E * Z) \quad .....(2)$$

Where,

Δ_{e2}: Output of Quarter Bridge Circuit
V_2: Input Voltage to Quarter Bridge Circuit 2

$$C_2 = V_2 \frac{R_1 * R_3}{(R_1 + R_2) * (R_3 + R_4)} * GF$$

d_2 : Distance Between Force F_{xy} and Strain Gauge B

Equations (1) and (2) can be rearranged as follows if $V_1 = V_2$, i.e. if $C_1 = C_2$, then

$$\begin{aligned} \Delta_{e1} - \Delta_{e2} &= F_{xy} * C_1 * (d_1 - d_2) /(E * Z) \\ &= F_{xy} * C_1 * d /(E * Z) \end{aligned}$$

i.e.,

$$\begin{aligned} F_{xy} &= (\Delta_{e1} - \Delta_{e2}) * E * Z /(C_1 * d) \\ &= C_{11} * (\Delta_{e1} - \Delta_{e2}) \quad .....(3) \end{aligned}$$

Where,
C_{11} = constant

Substituting the value of F_{xy} thus obtained in equation (1) determines the value of d_1 which in turn determines the offset Δ_y.

The force F_{xz} generates a torque about y axis. The cross section of finger being rectangular in shape, this torque tries to twist the finger.

It is well known [32] for rectangular cross section that

$$T_y = G * \gamma * (a * b * b) / (3 + 1.8 * b / a)$$

Where,

T_y : Torque due to F_{xz}

γ : Shear Stress Produced by T_y

G : Shear Modulus

Since,

$$G = \frac{E}{2(1 + \mu)};$$

The output of quarter bridge 3 for strain gauge C is given by following expression.

$$\Delta_{e3} = \frac{2.0 * F_{xz} * \Delta_z * (1 + \mu) * C_3 * (3 + 1.8 * b / a)}{a * b * b * E} \quad .....(4)$$

Where,

Δ_{e3}: Output of Quarter Bridge Circuit

μ : Poisson's Ratio

a : Larger Side of Cross Section of Gripper Finger

b : Smaller Side of Cross Section of Gripper Finger

V_3 : Input Voltage to Quarter Bridge Circuit 3

F_{xz}: Grip Force with Δ_z offset

and,

$$C_3 = V_3 \frac{R_1 * R_3}{(R_1 + R_2) * (R_3 + R_4)} * GF$$

$$\text{i.e. } \Delta_z = \frac{\Delta_{e3} * a * b * b * E}{2.0 * F_{xz} * (1 + \mu) * (3 + 1.8 * b / a) * C_3}$$

$$= C_{33} * \Delta_{e3} \quad (\text{As } F_{xz} = F_{xy}) \quad .....(5)$$

Where,

C_{33} = constant

C_1, C_2 and C_3 in expressions 1, 2 and 4 are constants. Equation (3) gives the magnitude of grip force F_x (= F_{xy} = F_{xz}). Equations (1) (or equation (2)) and (5) gives the y and z offsets, Δ_y and Δ_z of grip force respectively.

The output of the quarter bridge 4 is directly proportional to the bending strain of gauge D due to moment generated at contact points between finger pad and object in inaccurate grasping.

As in the case of bridge 1 we have for strain gauge D bridge 4 output is as follows,

$$\Delta e_4 = M_d * C_4 / (E * Z) \qquad .....(6)$$

Where,

$$C_4 = V_4 \frac{R_1 * R_3}{(R_1 + R_2) * (R_3 + R_4)} * GF$$

V_4 : Input Voltage to Quarter Bridge Circuit 4

$$\text{i.e. } M_d = \Delta e_4 * E * Z / C_4$$
$$= C_{44} * \Delta e_4 \qquad .....(7)$$

Where,

C_{44} = constant

The signed quantity M_d, the moment at strain gauge D is the reflection of error in pitch of the gripper.

BRIDGE POWER SUPPLY

The voltage applied to a strain gauge bridge creates a power loss in each arm, all of which must be dissipated in the form of heat. This causes the sensing grid of every strain gauge to operate at a higher temperature than the substrate to which it is bonded. This affects the gauge performance. Following factors determine the optimum excitation level of any strain gauge application.

1. Strain gauge grid area (Active gauge length x active grid width).
2. Gauge resistance.
3. Heat sink properties of the mounting surface.
4. Environmental operating temperature range of the gauge installation.
5. Installation and wiring technique.

The bridge excitation voltage for our application is selected from Grid Power Density Curves [33]. Selecting the most appropriate power-density lines of the chart depends, primarily upon two considerations: degree of measurement accuracy required, and substrate heat-sink capacity.

ELECTRICAL AND MAGNETIC DISTURBANCES

Interfering voltages may be induced in the leads and measuring grids by electrical and magnetic disturbances. This influence can be substantially reduced when the individual cables are twisted and shielded. Twisting is the only practicable protection against magnetic disturbances [34], whilst shielding suppresses the influence of electrical disturbance.

FILTERING

In practical applications of the Wheatstone bridge in strain gauge measurements it is often helpful and advantageous to use filtering techniques in the signal conditioning stage to improve the results. When the static portion of signal is of main interest, but this part is submerged by a big noise level, a low pass filter can be used to improve the signal to noise ratio. If on the contrary, the dynamic portion of the signal is of interest but is practically hidden within a big d.c. part, decoupling can be achieved by introducing a high-pass filter. Most often a band pass filter is applied which allows concentration on the interesting frequency range. A low pass RC filter is incorporated in bridge circuitry for our application.

SIGNAL AMPLIFICATION

The output from a strain gauge bridge is a matter of millivolts. In order to use a commercially available A/D converter it is necessary to amplify this voltage to the order of 5000 for strain gauges A and B and to the order of 8000 for strain gauges C and D. Instrument amplifiers AD624, AD 524, AD625 and INA 256 WG which give adjustable gain to 10000 are used to achieve this. However, these instrument amplifiers are prone to drift.

If amplification = GAIN (Gain of amplifier), then the amplifier output

$$\Delta_{eami} = GAIN * \Delta_{ei}, \quad i = 1,4$$

For calculation purposes the analogue voltages need to be converted to digital equivalence. This shall be done using 12 bit A/D converter of Macintosh which gives an equivalence of +- 2047 (Decimal form) corresponding to 10 V input to the A/D converter.

A decimal form number in the computer Δ_{edi} is thus related to Δ_{eao} by

$$\Delta_{edi} = \Delta_{eami}/10*2047, \quad i = 1,4$$

It follows then that,

$$\Delta_{eami} = 2047/10*GAIN*\Delta_{edi}$$
$$= K*\Delta_{edi}$$

Where K is fixed constant.

DETERMINING ERROR VECTOR E_r

In Fig. 5 we introduce a graphical representation of local frames for gripper as well as for object. For proper grasp, the homogeneous transformations matrix T_r, describing object frame relative to gripper frame shall be a 4X4 unit matrix. In that case, local frame of object as well as that of gripper shall be superimposed on each other.

In case of improper grasp, in order to define T_r, we will need six quantities: three involving translation and three more involving rotation. The three translational quantities are Δ_{xerr}, Δ_{yerr} and Δ_{zerr} corresponding to three offsets and the three rotational quantities are $\Delta\theta_{err}$, $\Delta\phi_{err}$ and $\Delta\psi_{err}$ corresponding to error in roll, pitch and yaw orientation of gripper with respect to object.

We now define error vector E_r describing these six components as follows,

$$E_r = [\Delta_{xerr} \quad \Delta_{yerr} \quad \Delta_{zerr} \quad \Delta\theta_{err} \quad \Delta\phi_{err} \quad \Delta\psi_{err}]^T \quad .....(8)$$

These six quantities now.can be determined as follows:

DETERMINATION OF Δ_{xerr}, Δ_{yerr} AND Δ_{zerr}

To keep track of gripper opening between two fingers we have incorporated a potentiometer (Fig. 6). As the fingers move closer or away from each other, the potentiometer output voltage varies proportionately. The output voltage Δ_{epot} of potentiometer can be calibrated in terms of gripper opening. Let gripper opening be Δ_{xopt} when object is properly grasped between the fingers. If the potentiometer reading Δ_{e7} corresponds to Δ_x offset, then Δ_{xerror} given by following expression,

$$\Delta_{xerr} = \frac{\Delta_{xopt} - \Delta_x}{2} \quad .....(9)$$

Δ_{yerr} and Δ_{zerr} are given by following expressions,

$$\Delta_{yerr} = \frac{\Delta_{y1} - \Delta_{y2}}{2} \quad .....(10)$$

$$\Delta_{zerr} = \frac{\Delta_{z1} - \Delta_{z2}}{2} \quad .....(11)$$

Where, Δ_{y1} , Δ_{z1} and Δ_{y2} , Δ_{z2} are the y and z offsets indicated by strain gauges on first and second finger respectively.

DETERMINATION OF $\Delta\phi err$, $\Delta\theta err$ AND $\Delta\psi err$

The error in orientation (roll and yaw) (Fig. 7) is given by following expressions,

$$\Delta\phi err = \frac{\Delta_{y1} - \Delta_{y2}}{\Delta_x} \quad .....(12)$$

$$\Delta\psi err = \frac{\Delta_{z1} - \Delta_{z2}}{\Delta_x} \quad .....(13)$$

$$\Delta\theta err \sim M_{dopt} \doteq M_d \quad .....(14)$$

The value of $\Delta\theta$ corresponding to M_d has to be carried out by calibrating the strain gauge D.

Derivation of equations (9-14) is based on one assumption that while grasping an object contact is made on both the fingers simultaneously. However, in general, this need not be so. To get rid of this discrepancy, we propose following.

If the strain gauge readings show that contact is made only on one finger, the robot is directed to traverse the gripper assembly in appropriate x direction till a contact is made on another finger. This can be verified by signals received from the appropriate strain gauges. Let dx be the distance traversed by gripper assembly in order to have contact on another finger. Then we have,

$$\Delta_x = dx/2 ;$$

The value of Δ_x can now be substituted in equations (9-13) to find out various components of error vector E_r.

MODES OF GRASPING

Before deciding on the control algorithm based on our mathematical derivations it would be advantageous to figure out all possible modes of grasping the object between the gripper jaws. There are three possible modes of grasp as shown in Fig. 8.

Mode 1: This mode is shown in Fig. 8(a). In this case direction of local axes of object and those of gripper jaws are exactly the same. It is the most ideal and hence most rare case. This case being trivial will not be considered here.

Mode 2: In this case Fig. 8(b), the object is improperly grasped with certain output signals in appropriate bridges. This would be the most likely mode present in majority of the grasping problems.

Mode 3: In this case Fig. 8(c), there is a phase difference of 90 degrees between the local axes of object and gripper jaws. This situation is the most undesirable one.

Having discussed the modes of grasping we now examine how these various modes can influence the design of control algorithm.

SIGNAL PROCESSING

The strain gauge readings output by the sensor under load are related by following expression.

$$[F_{xz} \quad \Delta_y \quad \Delta_z \quad \Delta_\theta]^T = [C] \; [\Delta_e], \qquad \text{.....(15)}$$

Let $[H] = [F_{xz} \quad \Delta_y \quad \Delta_z \quad \Delta_\theta]^T$,

then,

$$[H] = [C] \; [\Delta_e]$$

Where [C] is a calibration matrix. The validity of equation (15) is based on two assumptions:

1. Linearity: The response of the strain gauges varies linearly with the applied load.

2. Superposition: The effect on each strain gauge reading due to F_{xz}, , Δ_y, , Δ_z and Δ_θ are additive.

The basic sensor calibration procedure consists of applying four known linearly independent $[H]_k$, k=1,4 and recording the resulting strain gauge readings $[\Delta_e]_{ij}$, i=1,4; j=1,4. The components of $[H]_{ki}$ and $[\Delta_e]_{ij}$ are denoted by $[h]_{ki}$, j = 1,4 and $[\Delta_e]_{ij}$,i = 1,4 respectively.

Then calibration matrix [C] can be obtained from following equation,

$$[C] = [\Delta_e]^{-1} * [H]$$

Once calibration matrix is computed error vector E_r can be found out to solve inverse kinematic problem to determine robot joint displacements to move the gripper at proper location and orientation.

EXPERIMENTAL SETUP

A microprocessor controlled gripper system is proposed as shown in Fig. 9 to carry out preliminary experiments. The circuits being used for amplifying various strain signals are as shown in Figs. 10-13. The problem of data processing required in conjunction with the sensors is overcome through the use of 'C' processor of Macintosh which is capable of handling complex data, computing error vector and storing the information fed in from the sensors. Modifications or addition to the control strategy can simply be carried out by altering the software.

Fig.15 shows the first experimental setup for calibrating strain gauges A, B and C. The face plate is screwed to the finger pad of the gripper and has a carefully marked grid on it as shown in Fig.16 and Fig.17. Grid plate once mounted on the finger pad defines the Y and Z co-ordinates of the grid nodes. Gripper fingers are loaded through a pressure plate, cable, dial gauge (to measure accurately the applied force) and a vice. The pressure plate has pointed cone at its center. The point of application of force on finger pad can be easily varied by locating this pointed cone at desired node points.

Using the experimental setup shown in Fig.15 the sensor response for various loads at Y and Z offsets is noted as shown in Figs. 18-31. Sensor response is measured at all nodes however, only representative examples are shown in Figs. 18-31. Fig.18-31 shows the the variation of strain gauge response as magnitude of force and offsets y and z changes. One more experimental setup for measuring the response of all strain gauges to bending moment in YZ plane is being made at the time of writing this final report. The strain gauges A, B and C can be calibrated using following procedure.

CALIBRATION

Let Δe $[\Delta e_1\ \Delta e_2\ \Delta e_3\ \Delta e_4]^T$ represent the strain gauge readings output by the sensor under load. Let F $[F\ \Delta_y\ \Delta_z\ \theta]^T$ be the force vector. Then F and Δe are related by

$$[F] = [C]\ [\Delta e] \qquad \ldots(16)$$

Where $[C] = (c_{ij})$ is a 4 x 4 calibration matrix.

The basic sensor calibration procedure consists of applying four known linearly independent sensor loadings F_k, k = 1,4 and recording the resulting strain gauge readings Δe_k. The components of F_k and Δe_k are denoted by f_{kj}, j = 1,4 and V_{ki}, i=1,4 respectively. The system of equations represented by equation (1) results in four equations for each row of (16). Since we have carried out only one set of experiment (for strain gauges A, B and C), we shall be using three equations for the data shown in Figs. 18-29. This system of equations can be solved using standard methods for solving simultaneous equations. Repeating this procedure for three rows yields a solution for 3 x 3 calibration matrix C. Once we carry out the second set of experiments, 4 x 4 calibration matrix can be carried out to compute error vector E_r as discussed earlier.

Up to this point we have ignored any possible bias in the sensor. In practice, each of the strain gauge will output a small non zero value under zero load. This value is a constant offset or DC shift which must be compensated for to accurately obtain experimental data. To account for this bias, the equation (1) is modified as follows.

$$[F] = [C]\ [\Delta e - B] \qquad \ldots(17)$$

The sensor bias B is obtained by reading the strain gauge output under zero load. Individual sensor bias is accounted in the data shown in Figs. 18-29.

CLOSURE

We have, in this report briefly discussed how a 3 x 3 calibration matrix can be computed from the response of the sensors taken for first experimental setup. One more experimental setup is being carried out to compute all elements of 4 x 4 calibration matrix C. This report has demonstrated that building a sensor system based upon strain gauges is possible for reorienting and locating parallel jaw gripper with respect to the object to be grasped and offers a reliable and mechanically rugged solution. The major steps involved in reorienting gripper with respect to object are as shown in Fig. 32. Experiments to test a control algorithm as shown in Fig. 32 are yet to be carried out.

+++

REFERENCES

1. Ruocco S.R. : "Robot Sensors and Transducers" John Wiley & sons, New York (1989).

2. Lestelle, D.: "Gripper with Finger Built-In Force / Torque Sensors", Proceedings of the 5th International Conference on Robot Vision and Sensory Controls, pp. 69-77, (1985).

3. Piller G. : "A Compact Six-Degree of Freedom Force/Torque Sensor For Assembly Robots", Proceedings of 12th International Symposium on Industrial Robots, 6th International Conference on Industrial Robot Technology, pp.121-129, (1982).

4. Yoshihiko Nakamura : "Design and Signal Processing of Tsuneo Yoshikawa; Six Axis Force Sensors", Ichiro Futamata Robotic Research, The Fourth International Symposium,(Ed. Bolles, R.C. and Roth, B.) pp. 75-81, (1987).

5. Bicchi, A. ; Dario, P. : "Intrinsic Tactile Sensing For Artificial Hands", Robotic Research, The Fourth International Symposium,(Ed. Bolles, R.C. and Roth, B.) pp. 83-90, (1987).

6. Oomichi, T.: "Mechanics and Multiple Sensory Bilateral Miyatake, T. Control of a Fingered Manipulator", Aekawa, A. Hayashi, Robotic Research, The Fourth International Symposium,(Ed. Bolles, R.C. and Roth, B.)pp. 145-153, (1987).

7. Nevins, J.L.; Whitney, D.E. : "Assembly Research", Tutorial on Robotics Second Edition Lee, C.S.; Gonzalez, R.C.; Fu, K.S. pp. 39-57.

8. "Force Sensing and Control", Tutorial on Robotics Second Edition Lee, C.S.; Gonzalez, R.C.; Fu, K.S. Chapter six PP. 323-326.

9. "Use of Sensors in Programmable Automation", Tutorial on Robotics Second Edition
Lee, C.S.; Gonzalez, R.C.; Fu, K.S.
pp. 327-338.

10. Shimano, B.; Roth, B. : "On Force Sensing Information and it's Use In Controlling Manipulators", Proceedings of the Eight International Symposium on Industrial Robots, pp. 119-126.

11. Paul, R.; Shimano, B.:"Compliance and Control"' Proceedings of the Joint Automatic Control Conference, pp. 694-699, (1976).

12. Whitney, D.E.: "Force Feedback Control of Manipulator Fine Motions", Journal of Dynamic Systems, Measurement and Control, pp. 353-359, (1977).

13. Mason, M.T.: "Compliance and Force Control for Computer Controlled Manipulators", IEEE Transactions on System, Man and Cybernetics, Vol. SMC-1, No. 6 pp. 418-432, (1981).

14. Raibert, M.H.: "Hybrid Position / Force Control of Craig, J.J. Manipulators", ASME Journal of Dynamic Systems, Measurement and Control, Vol. 102, pp.126-133, (1981).

15. Salisbury, J.K. : "Active Stiffness Control of A Manipulator in Cartesian Coordinates", Proceedings of th 19th IEEE Conference on Decision and Control. pp. 95-100, (1980).

16. Chi-Haur Wu; Paul, R. :"Resolved Motion Force Control of Robot Manipulator", IEEE Transactions on System, Man and Cybernetics, Vol. SMC-12 No. 2,pp. 266-275, (1982).

17. Cutkosky, M.: "Grasping As A Contact Sport",
Prasad Akella
Howe, R.;Imin Kao
Robotic Research, The Fourth International Symposium,(Ed. Bolles, R.C. and Roth, B.) pp. 199-206, (1987).

18. Martin, K.F:"Force Sensing in Magnitude, Direction Lockman, H. and Position", Trans. ASME VOl. 109, pp. 286-290. (1987).

19. Cutkosky, M.R.; Wright, P.K. : " Position Sensing wrists For Industrial Manipulators", Proceedings of 12th International Symposium on Industrial Robots, 6th International Conference on Industrial Robot Technology, pp.427-438, (1982).

20. Dillman, R. :"A Sensor Controlled Gripper With Tactile and Non-Tactile Sensor Environment", Proceedings of the 2nd International Conference on Robot Vision and Sensory Controls, pp. 159-170, (1982).

21. Williams, D.F.; Allen, D.M. ;"A Remote On-Line Technique For Accurate Robot Programming Employing Combined Tactile and Visual Sensing", Proceedings of the 2nd International Conference on Robot Vision and Sensory Controls, pp. 391-398, (1982).

22. Nguyen V. :"Constructing Force-Closure Grasps", Proceedings of 1986 IEEE International Conference on Robotics and Automation,Vol. III, pp. 1368-1373, (1986).

23. Cunningham, R.; Brooks, T.; Dotson, R.:" Smart Force/Torque Sensing Systems For Robots", Preprint from the Proceedings of the ASME Second International Computer Engineering Conference, (1982).

24. Watson, P.C; Drake,S.H. :"Pedestal and Wrist Force Sensors for Automatic Assembly", Proceedings of the 5th International Symposium on Industrial Robots, (1975).

25. Kozo Ono, Yotaro H. :"A New Design For 6-Component Force/Torque Sensors"; Mechanical Problems in Measuring Force and Mass. Martinus Nijhoff Publishers, Dordrecht. pp. 39-48. (1986).

26. Gerelle, E.:"Force Feedback Control", Proceedings of the 8th International Symposium on Industrial Robots, pp. 194-205, (1978).

27. Masuo Kasai at al:"Trainable Assembly System With An Active Sensory Table Possessing 6 Axes", Proceedings of the 11th International Symposium on Industrial Robots, pp. 393-404, (1981).

28. Van Brussel H. at al:"Further Developments of the Active Adaptive Compliant Wrist (AACW) for Robot Assembly", Proceedings of the 11th International Symposium on Industrial Robots, pp. 377-384, (1981).

29. Teoh, W.; Workman, G.L.: "Intelligent Gripper With Force Stiles, D. Feedback", Chu, Y.N. Proceedings of the 3rd International Conference on Robot Vision and Sensory Controls, pp. 385-388, (1983).

30. Parker, J.K. : "Position and Force Control When Positioning Objects With Robot Hands", IEEE International Conference on Robotics and Automation, Vol. I, pp. 35-40, (1986).

31. Murray, W.M.:"Strain Gage Techniques: Fundamentals and Stein, P.K. Applications", Vol. II, MIT, Cambridge, Mass., p. 304, (1956).

32. Singer, F.L.:"Strength of Materials", Harper and Brothers Publishers, New York, p.69, (1951).

33. "Optimizing Strain Gage Excitation Levels", Measurement Group Tech Note TN-502, Measurements Group, Inc., Raleigh, North Carolina.

34. Mardiguian, M. :"How to Control Electrical Noise"

+++

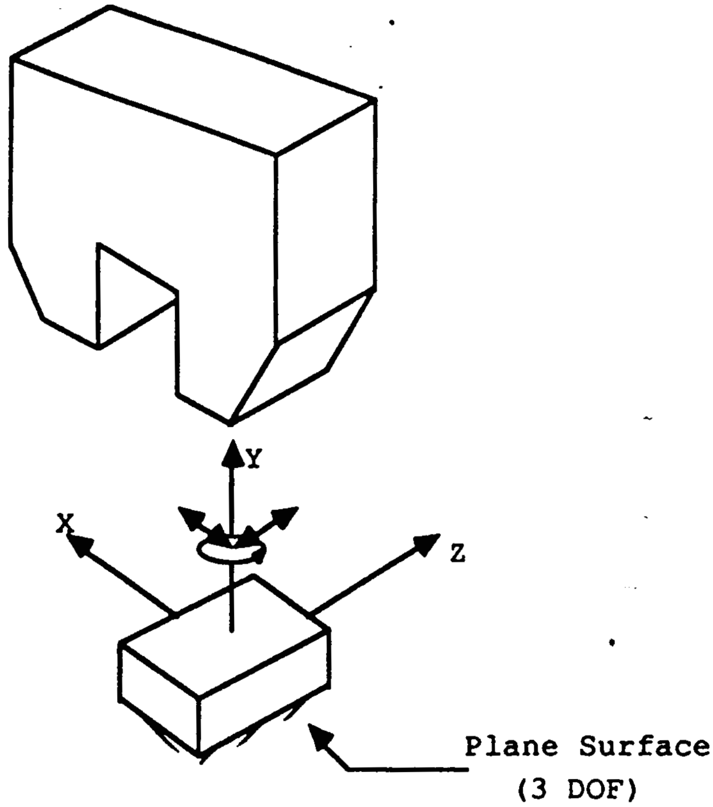

(a) Industrial Application

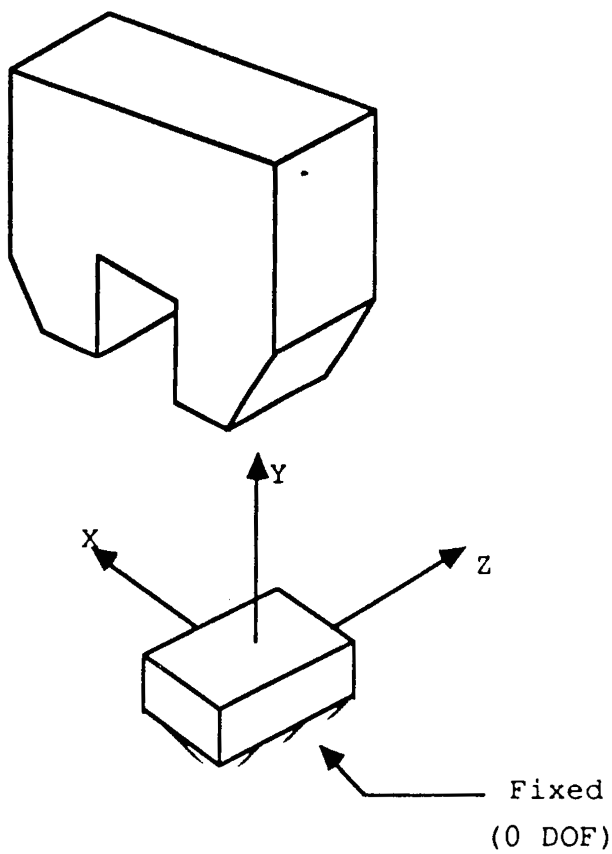

(b) Application In Space

FIG. 1
GRIPPER OBJECT INTERACTION

ORIGINAL PAGE
BLACK AND WHITE PHOTOGRAPH

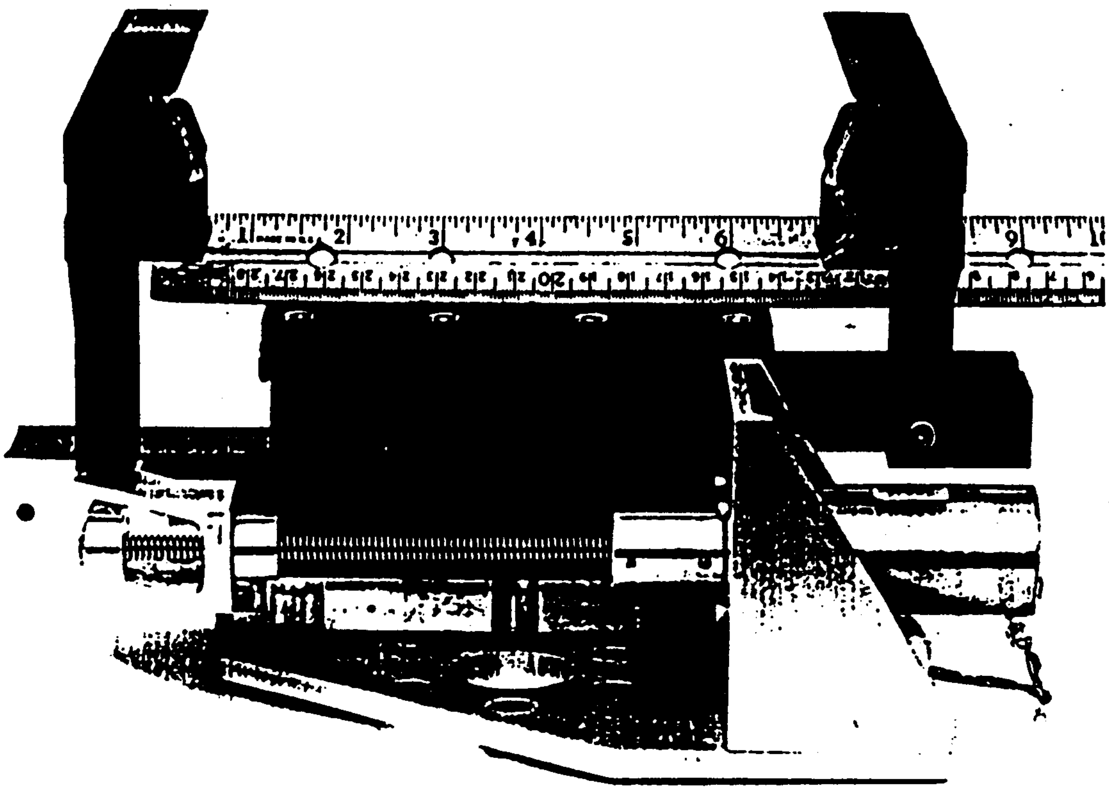

(a) Front View

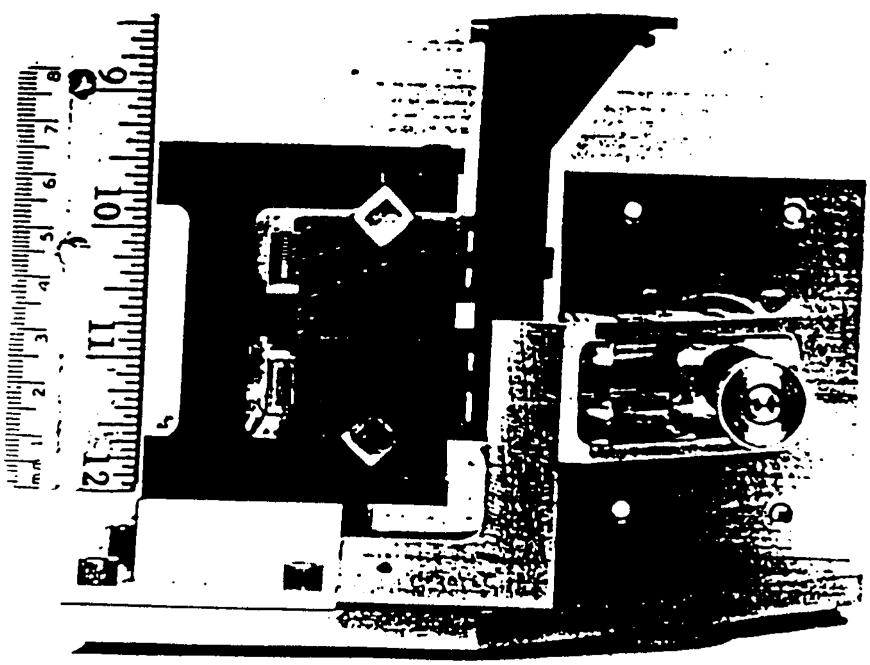

(b) End View

FIG. 2

THE GRIPPER

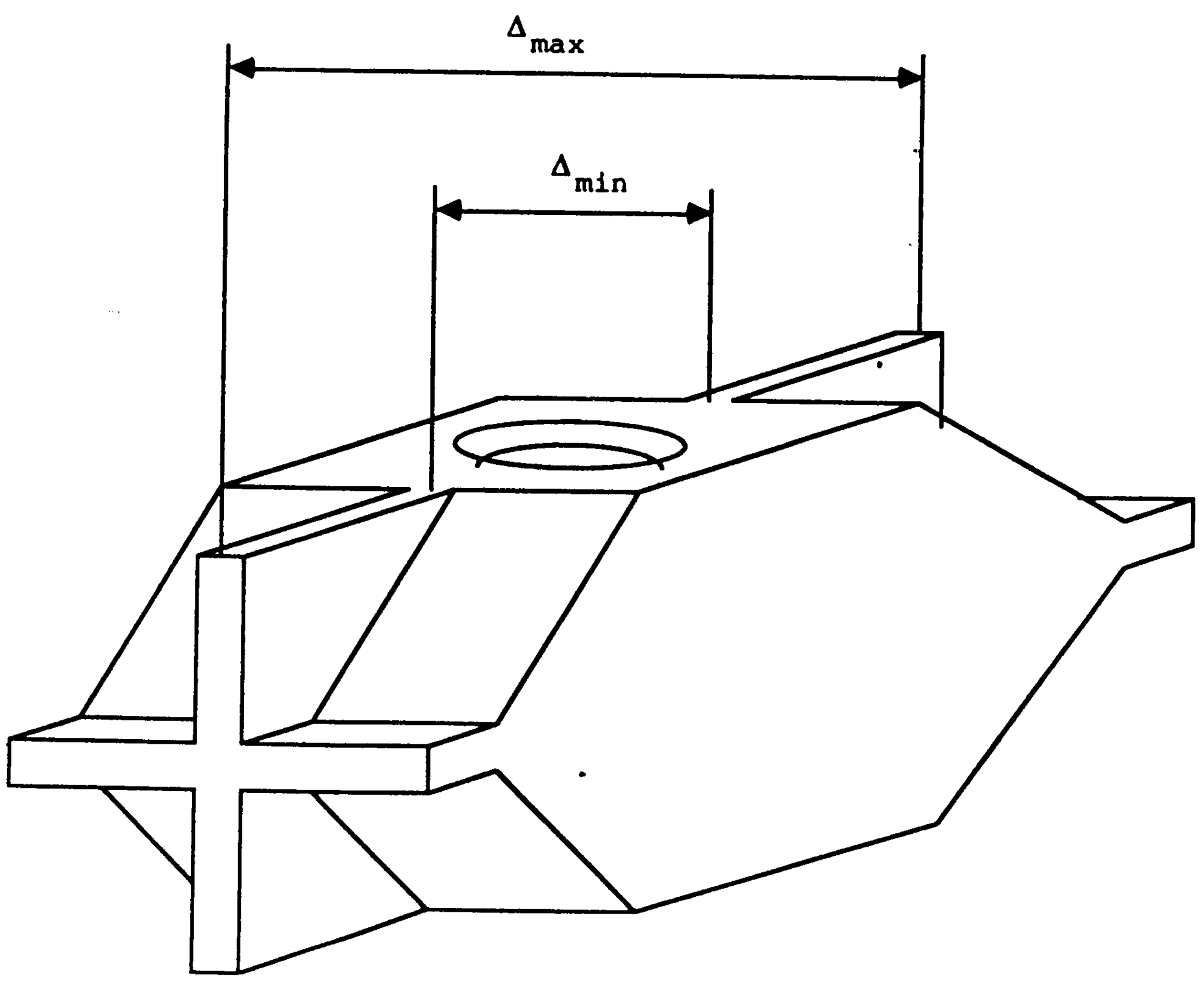

FIG. 3

OBJECT GEOMETRY

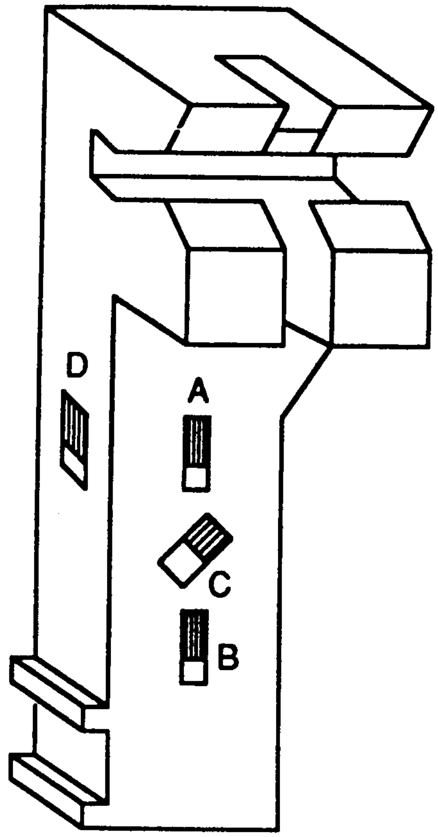

(a)

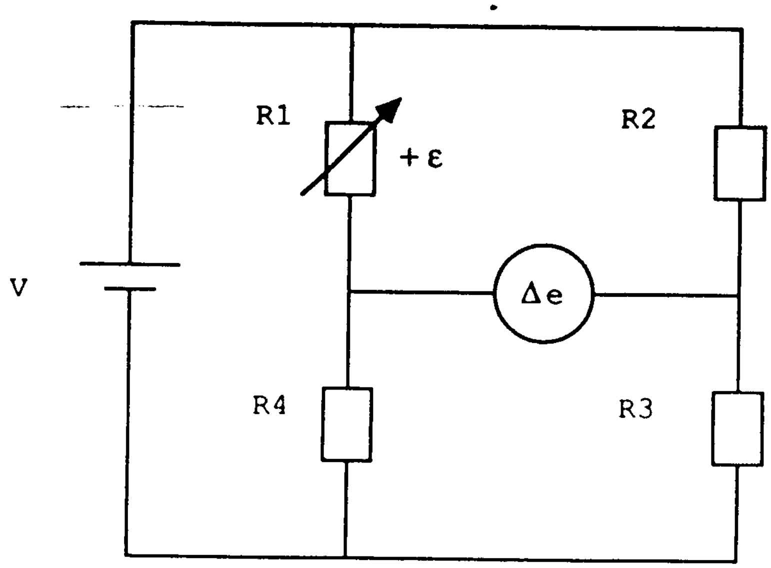

(b)

FIG. 4

LOCATION OF STRAIN GAUGES AND QUARTER BRIDGE CIRCUIT

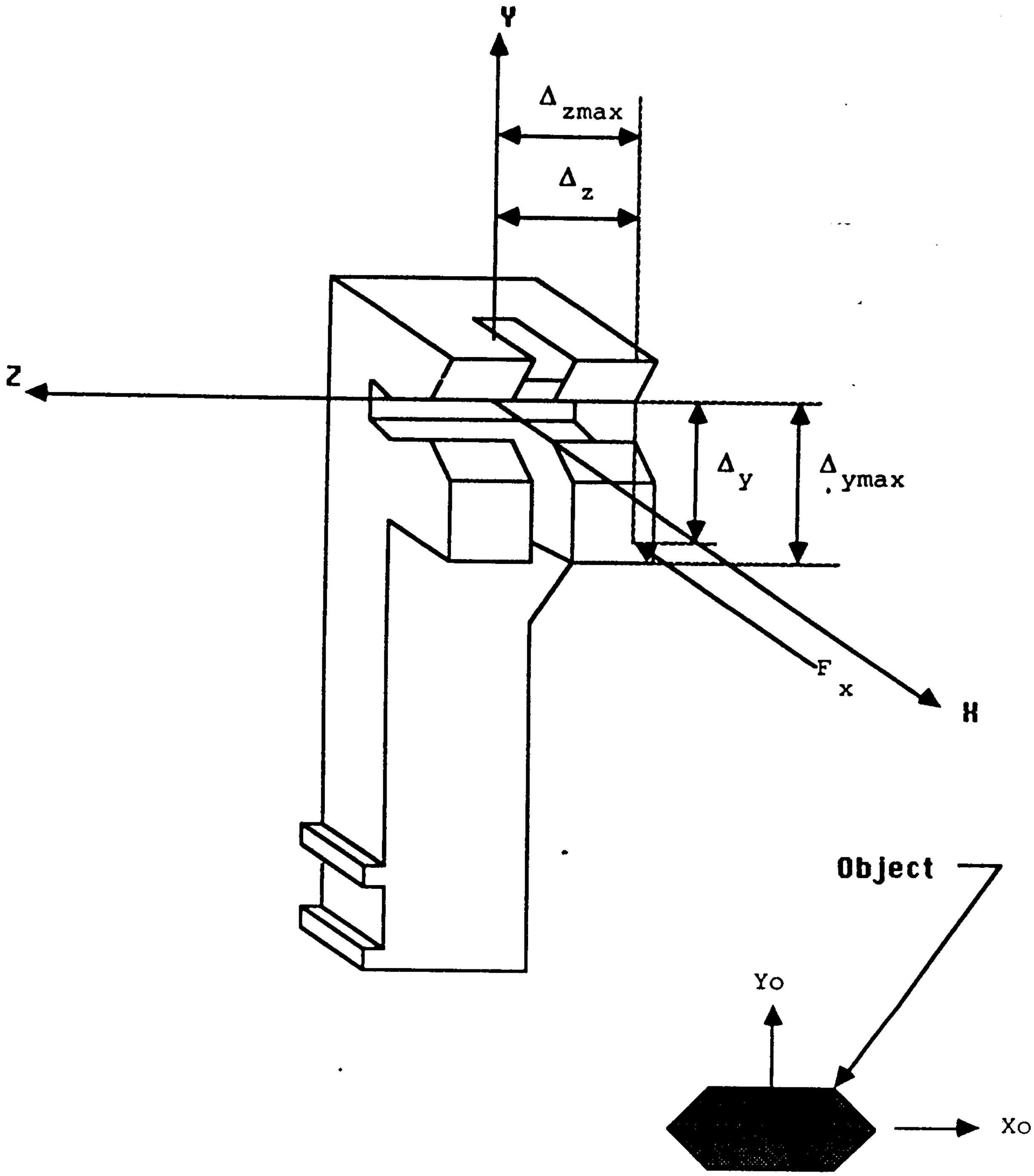

FIG. 5

LOCATION OF GRIP FORCE

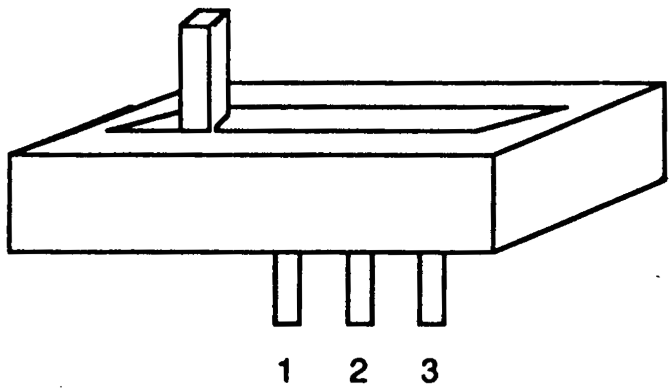

Physical Constructionn

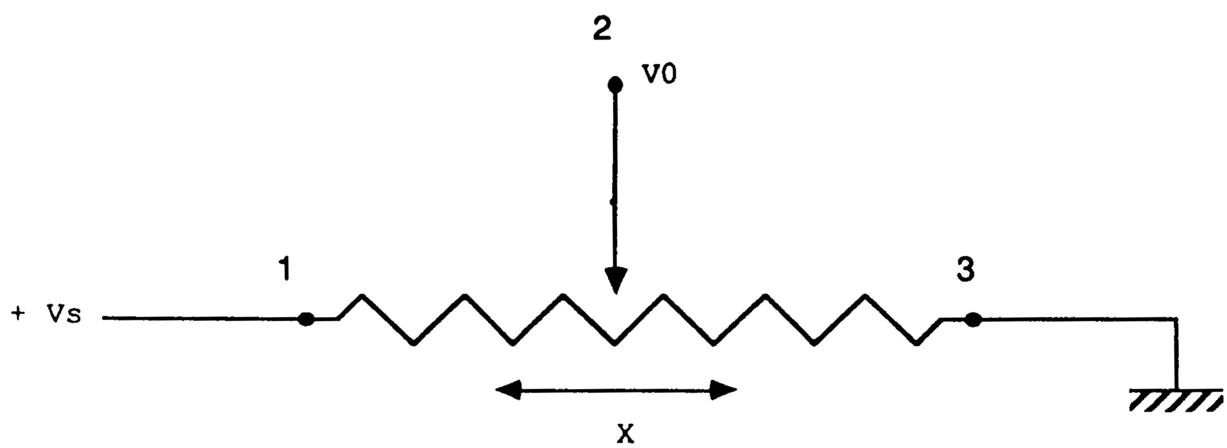

Schematic Representation

FIG. 6 GRIPPER OPENING MEASUREMENT USING A POTENTIOMETER

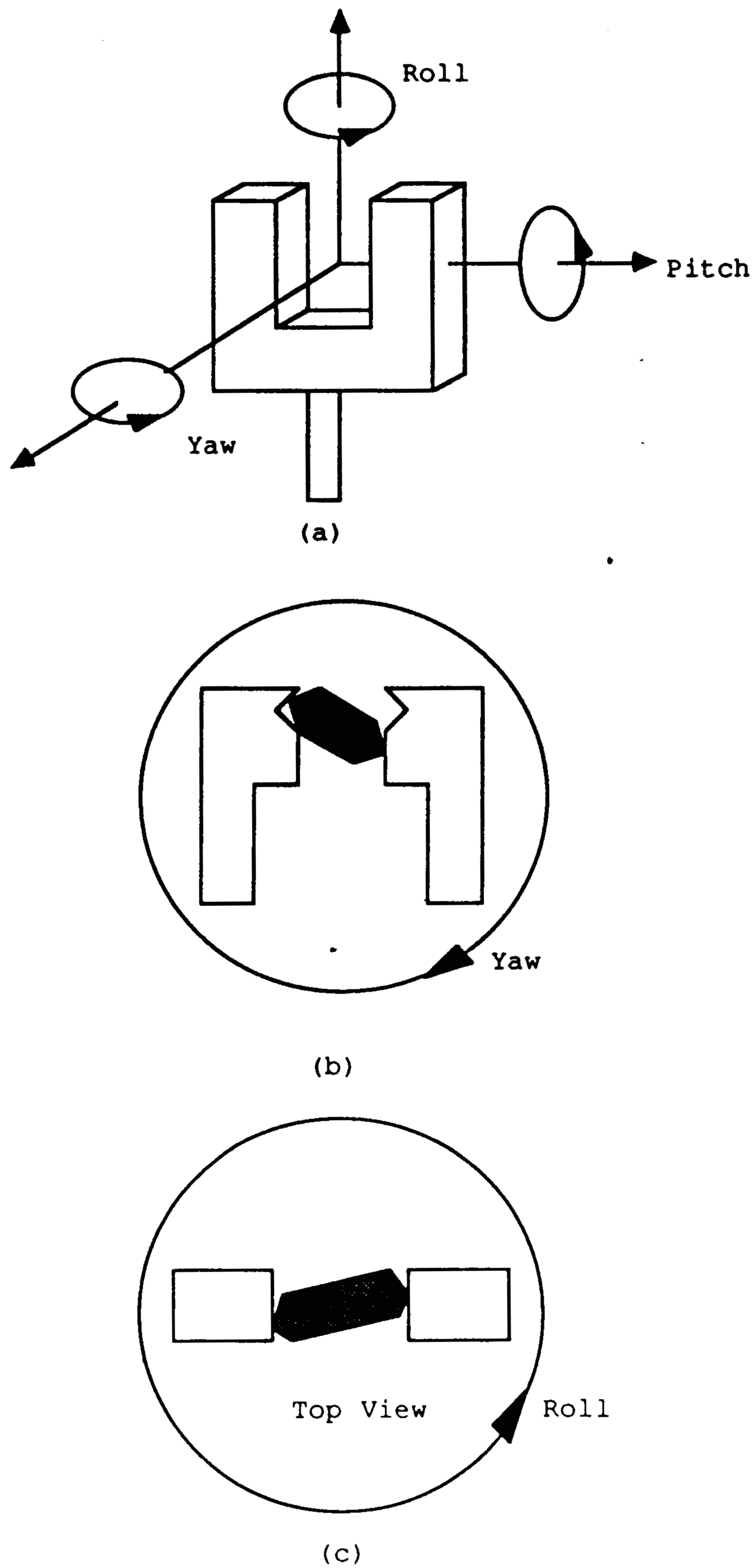

FIG. 7
DETERMINATION OF ROLL AND YAW ERROR

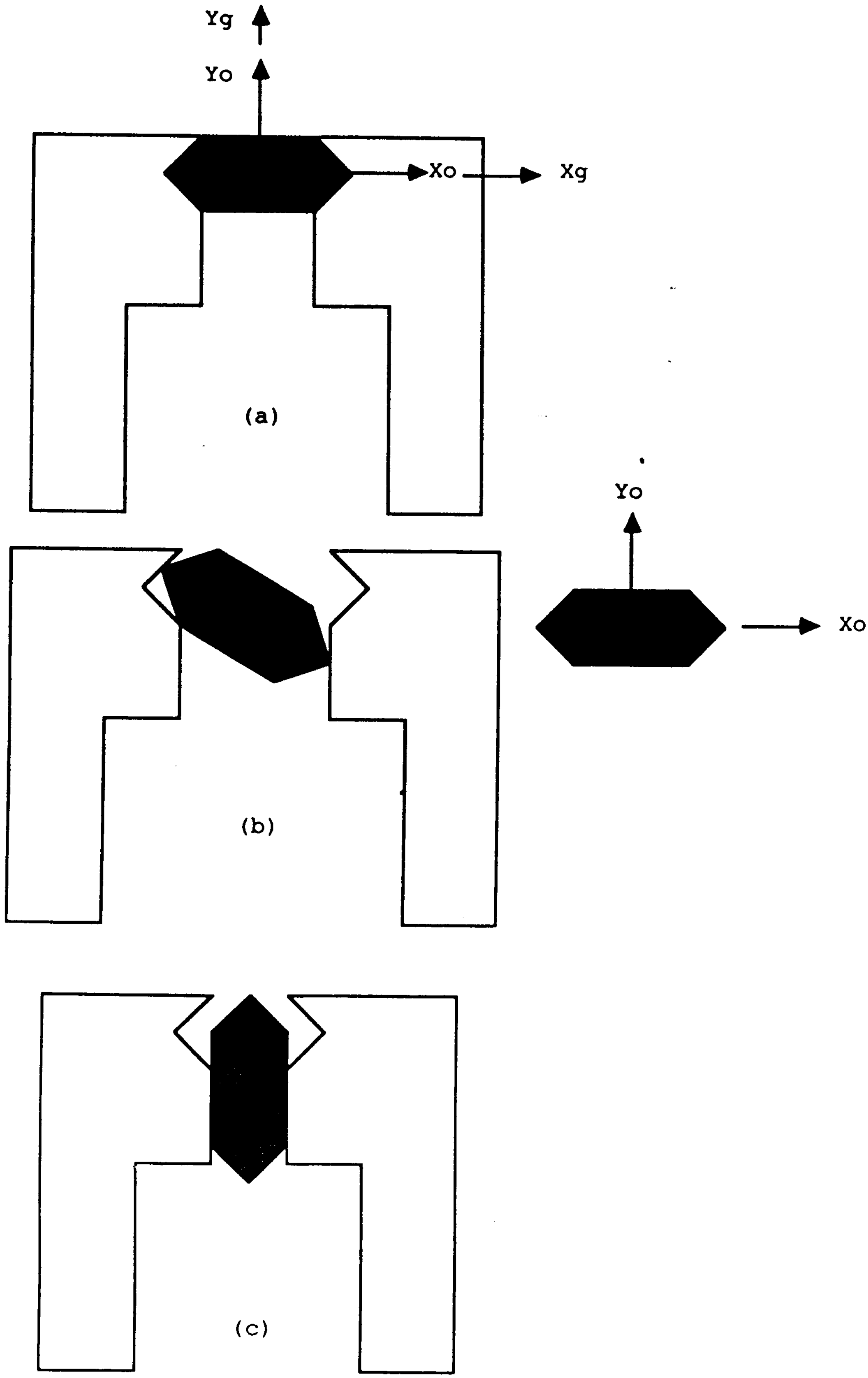

FIG. 8
DIFFERENT MODES OF GRASPING

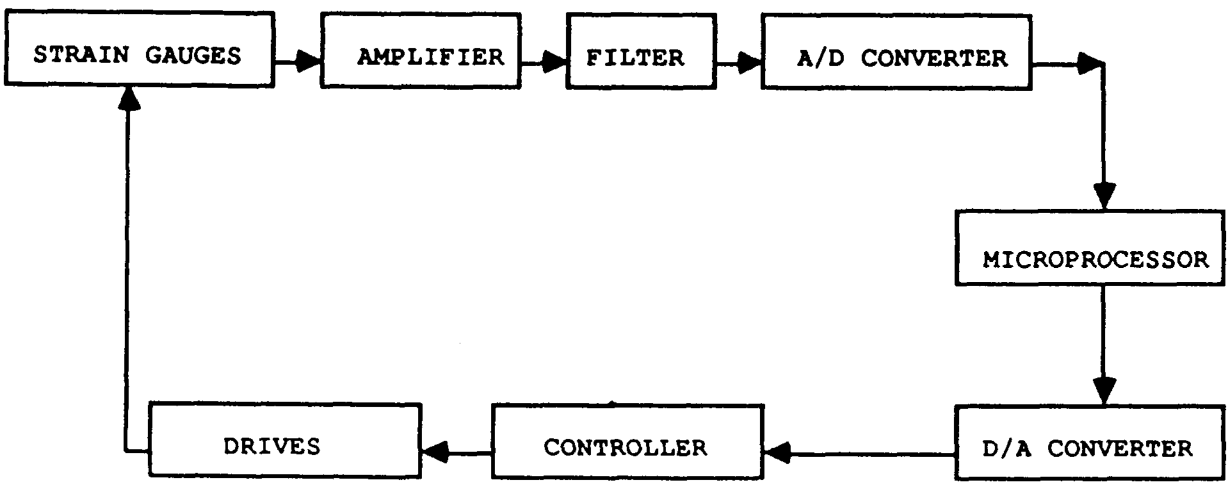

FIG. 9

SYSTEM HARDWARE

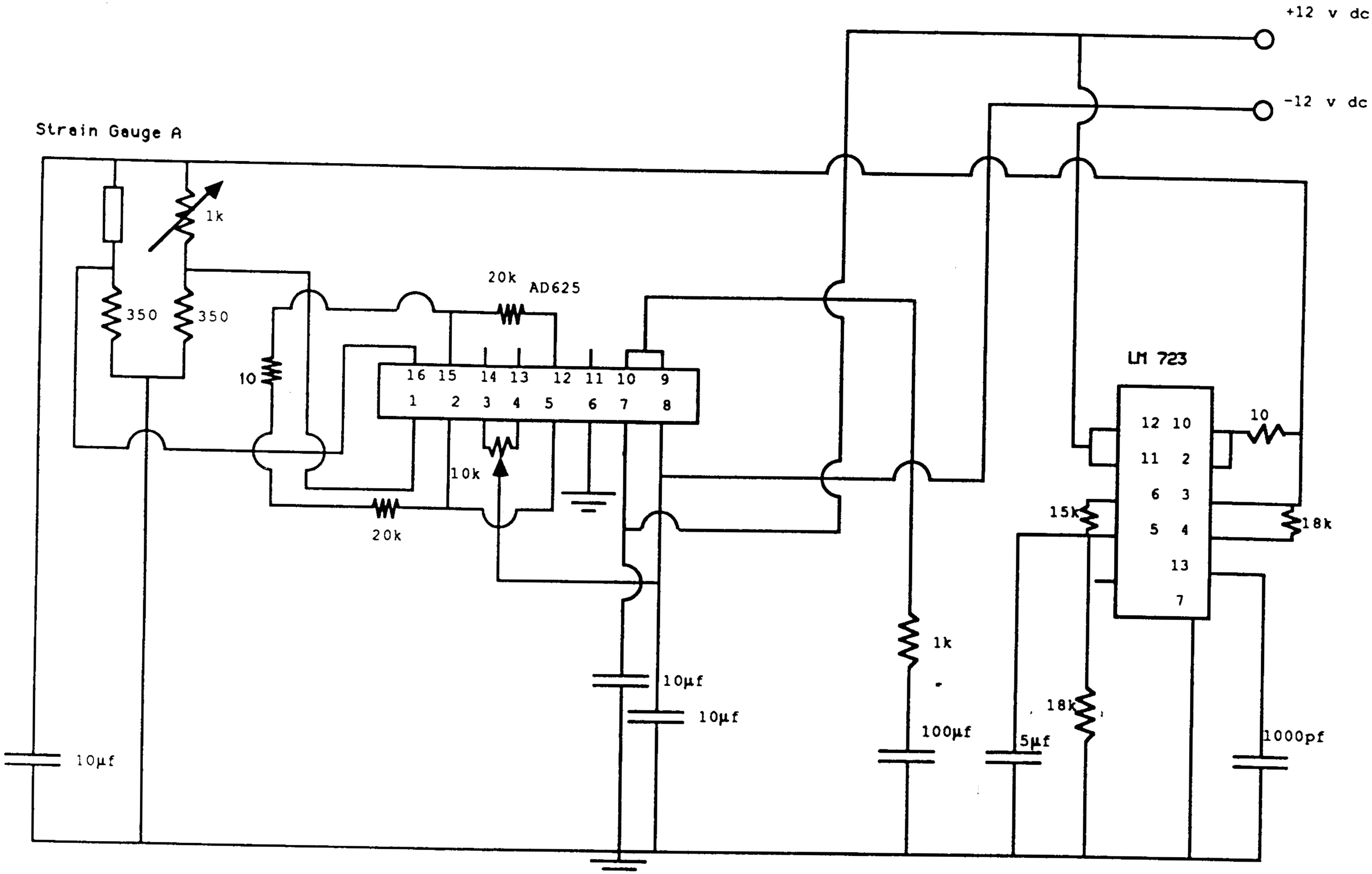

FIG. 10

CIRCUIT FOR STRAIN GAUGE A

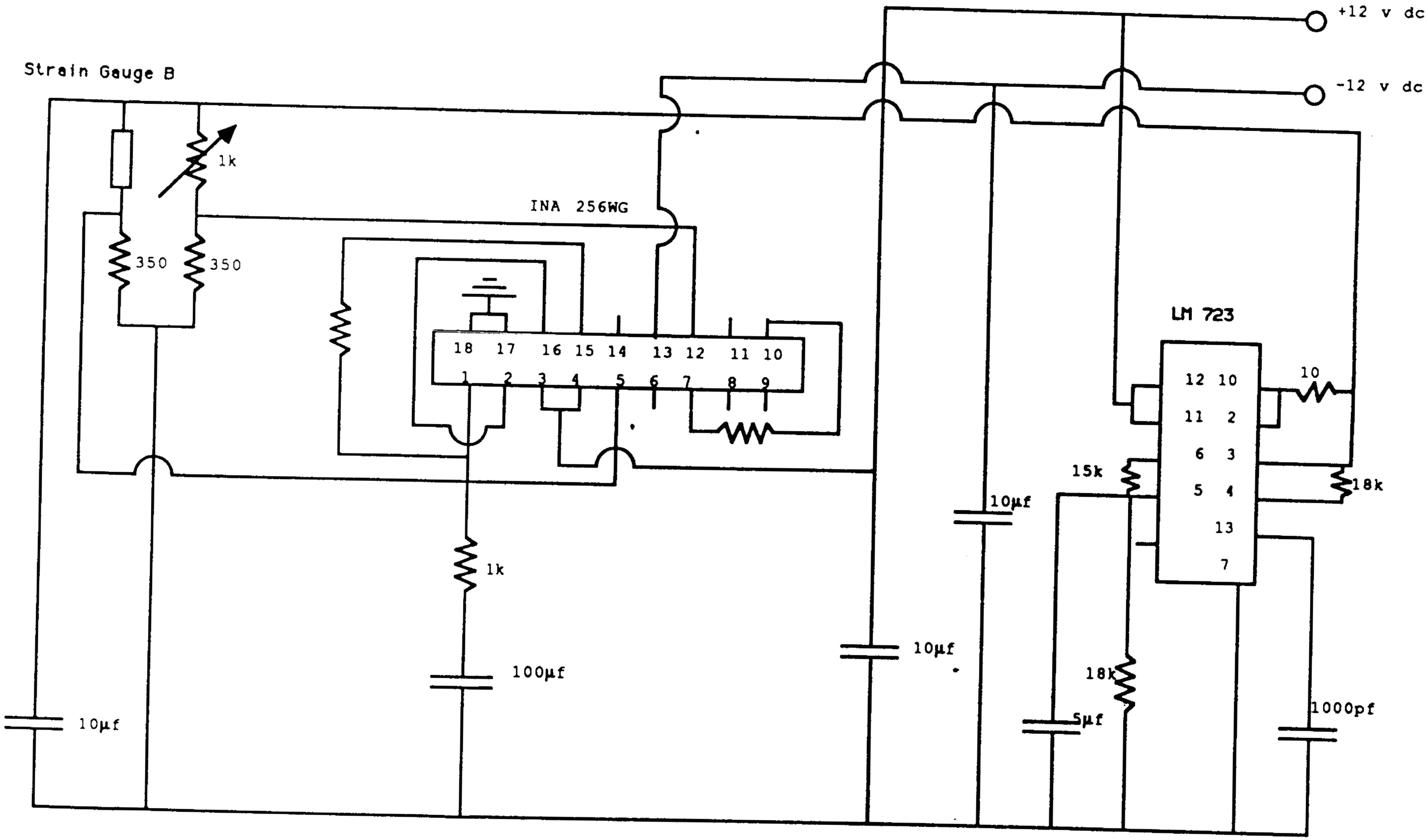

FIG. 11

CIRCUIT FOR STRAIN GAUGE B

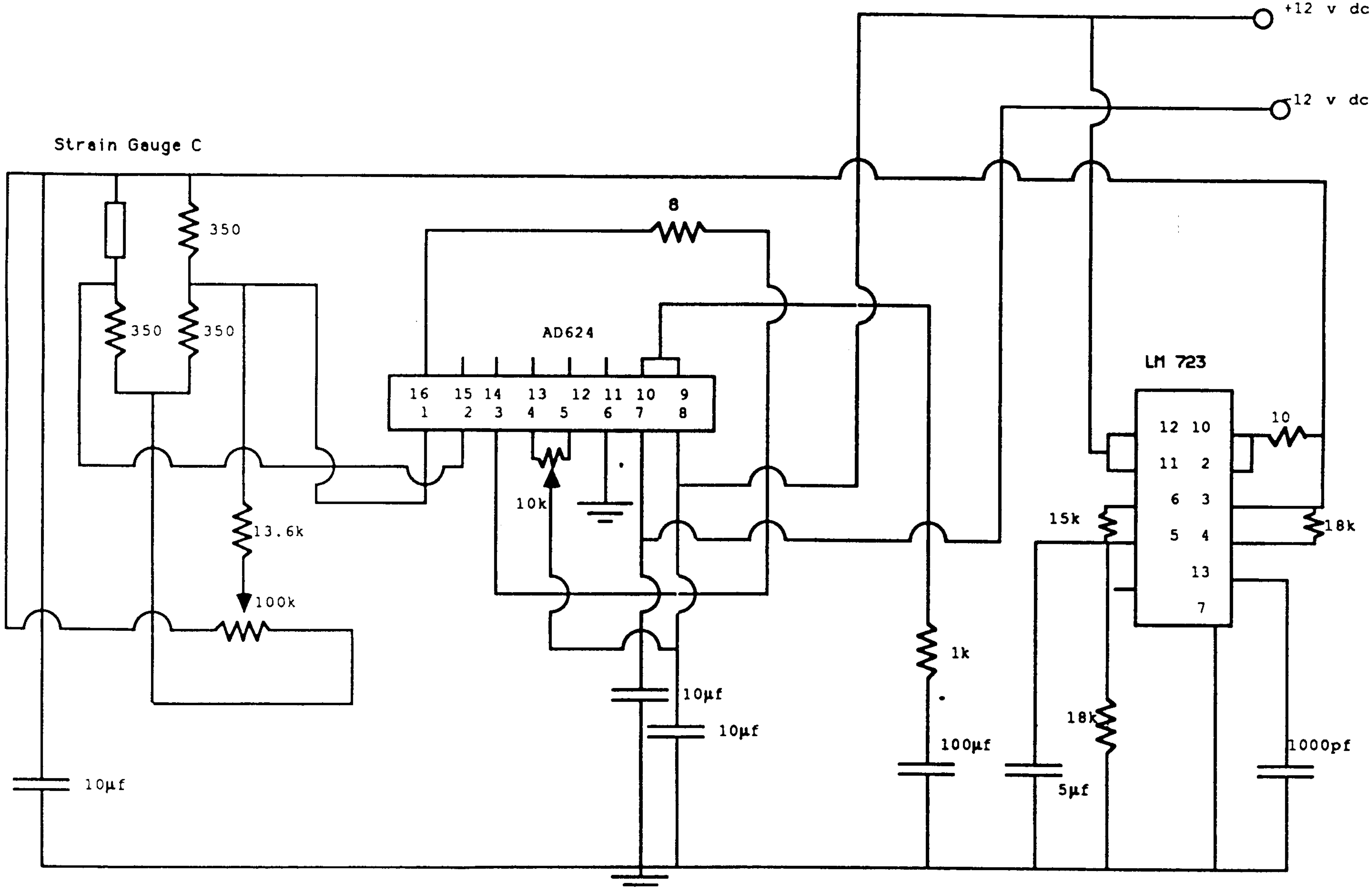

FIG 12

CIRCUIT FOR STRAIN GAUGE C

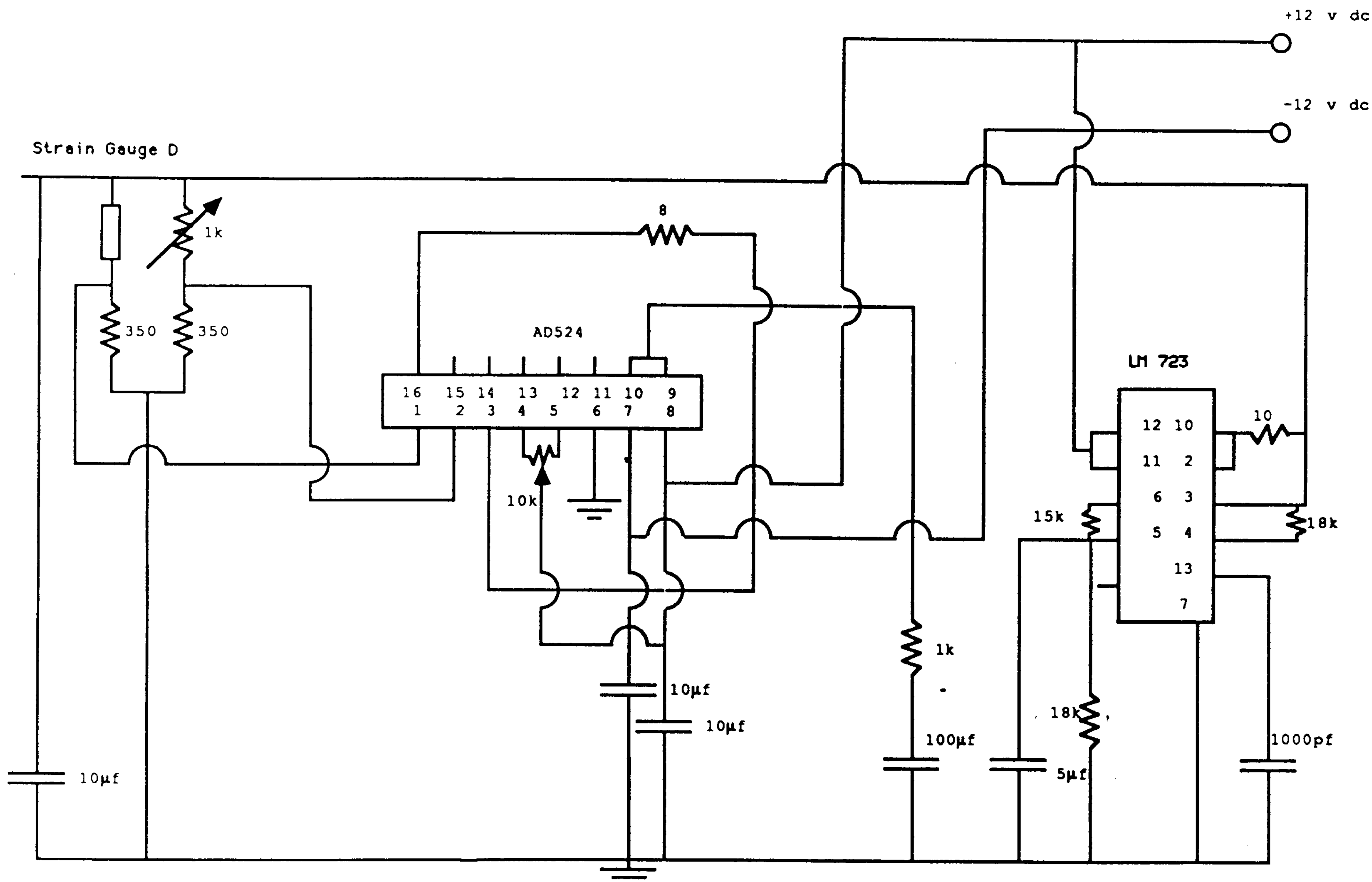

FIG 13

CIRCUIT FOR STRAIN GAUGE D

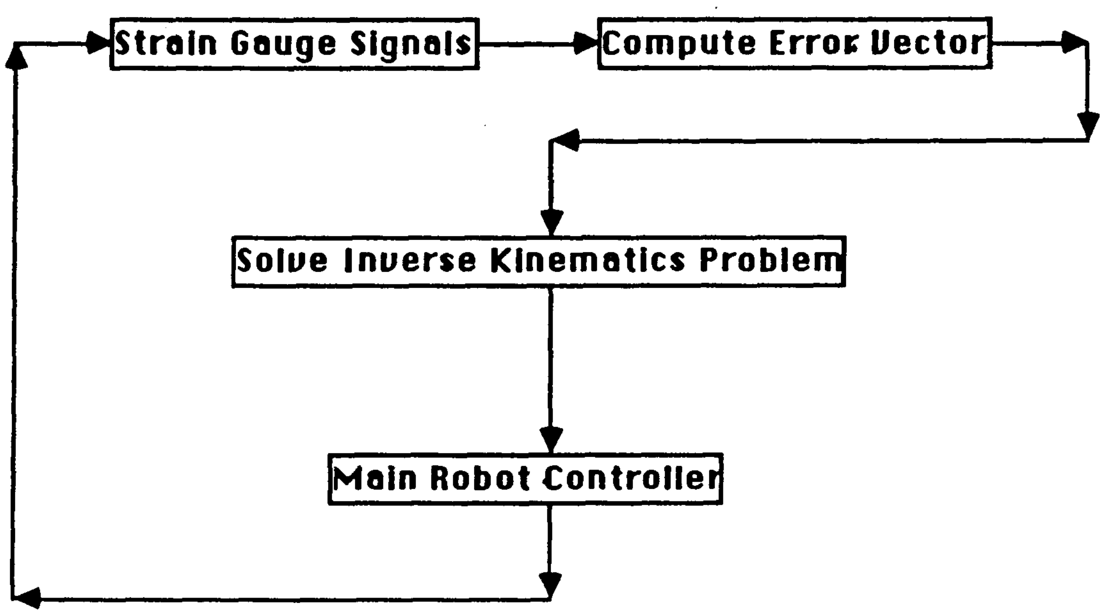

FIG. 14

CLOSE LOOP CONTROL OF GRIPPER

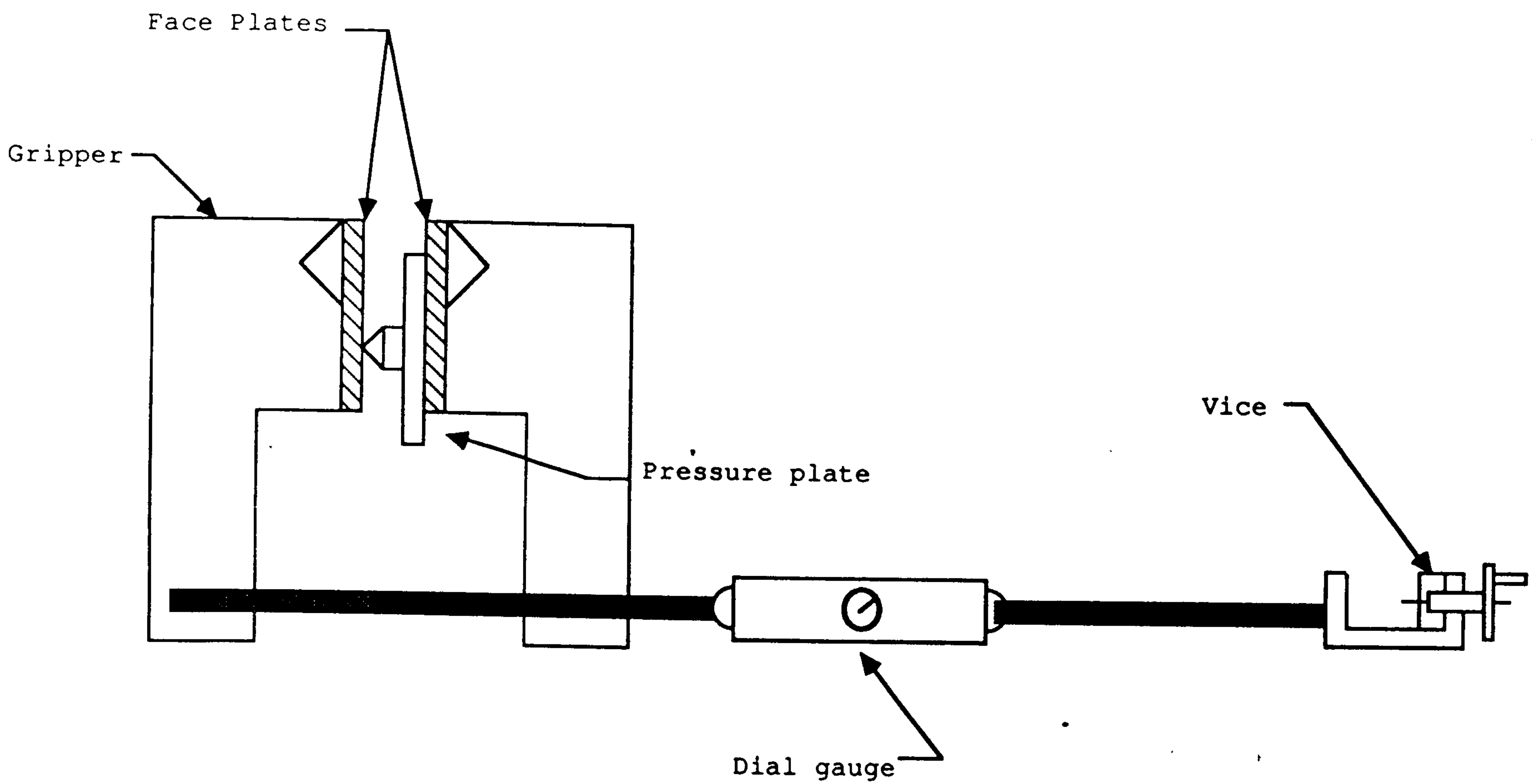

FIG. 15

THE EXPERIMENTAL SET-UP

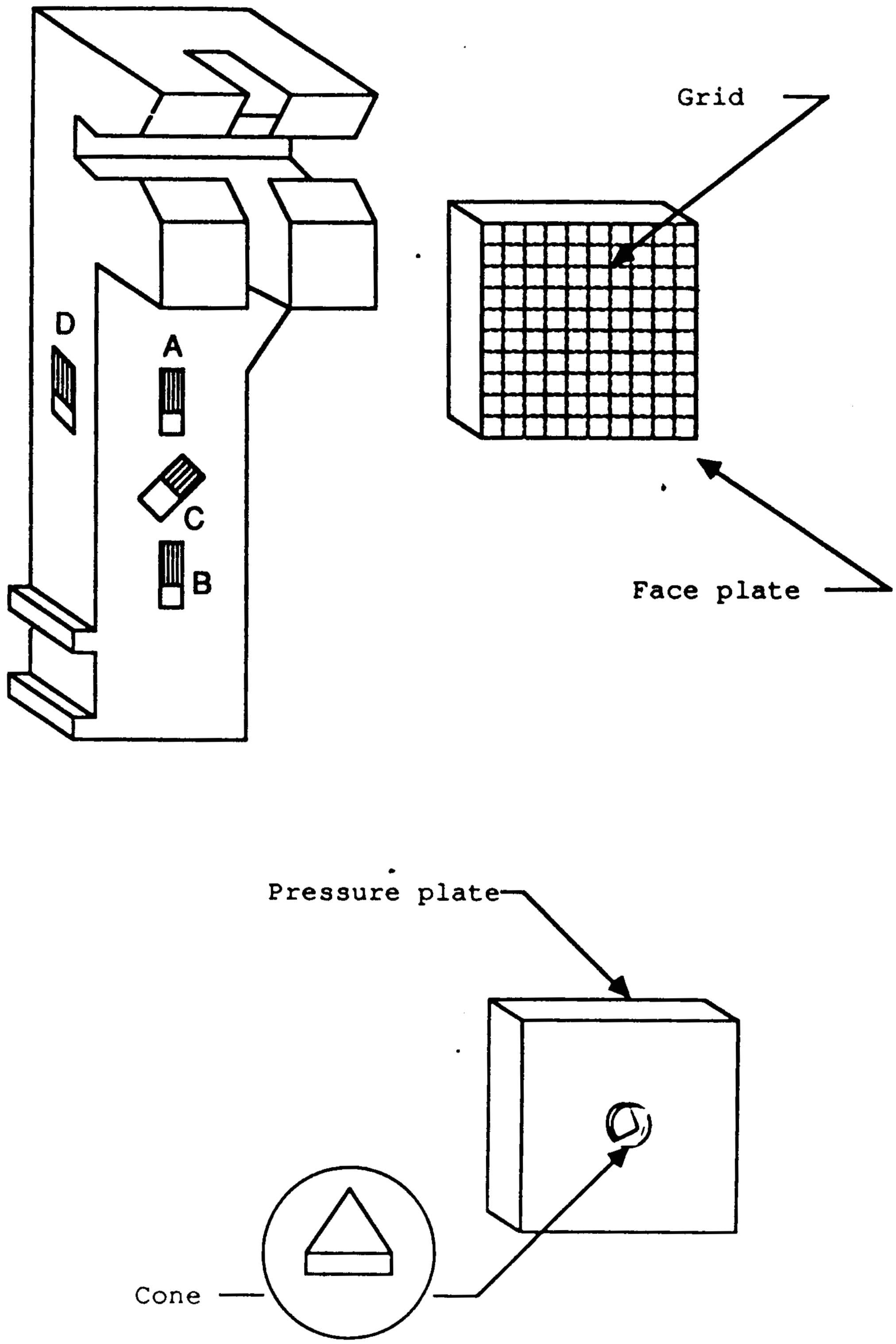

FIG. 16
Face & Pressure Plate For Finger Pad

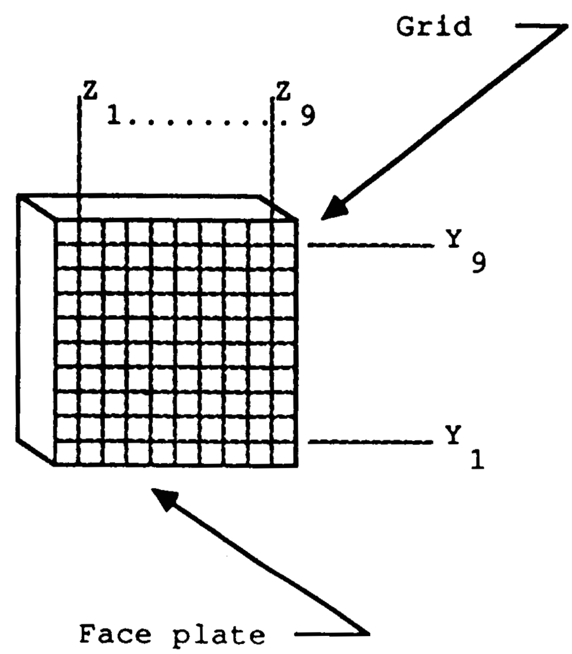

FIG. 17
Details of Face Plate Grid

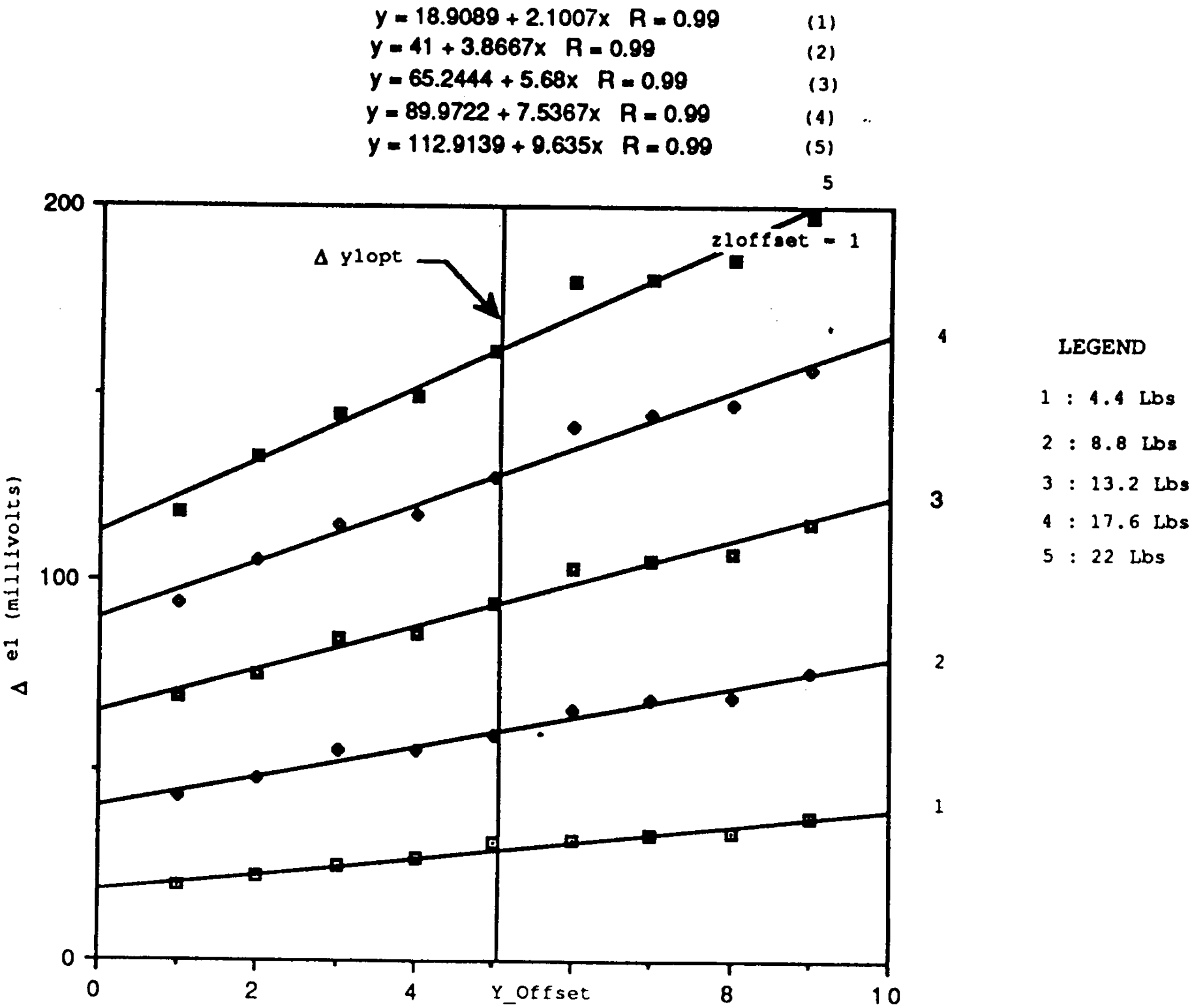

FIG. 18 Sensor Response Δe_1 V/S Δy_1 (Δz_1 = 1)

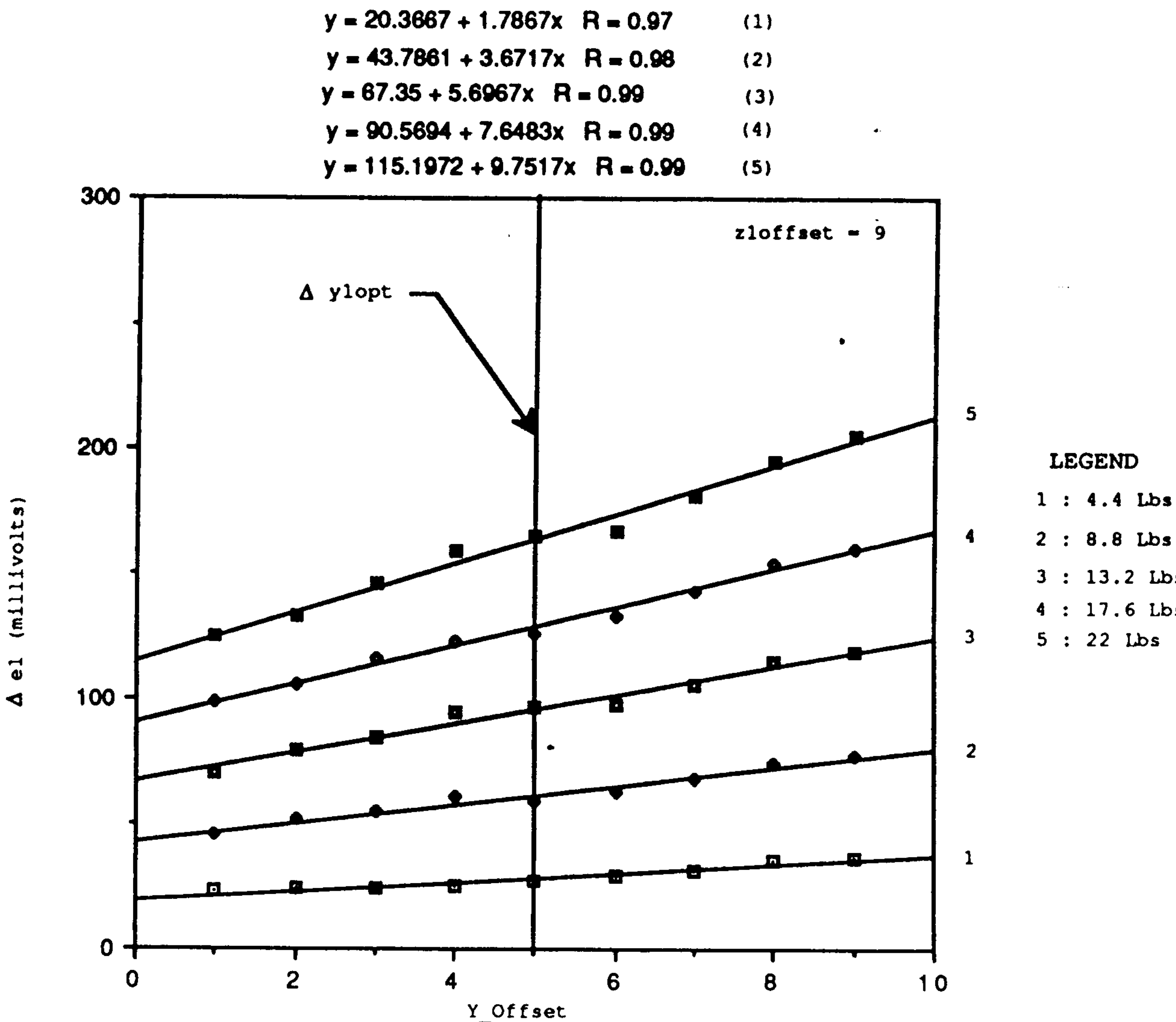

FIG. 19 Sensor Response Δe_1 V/S Δy_1 (Δz_1 = 9)

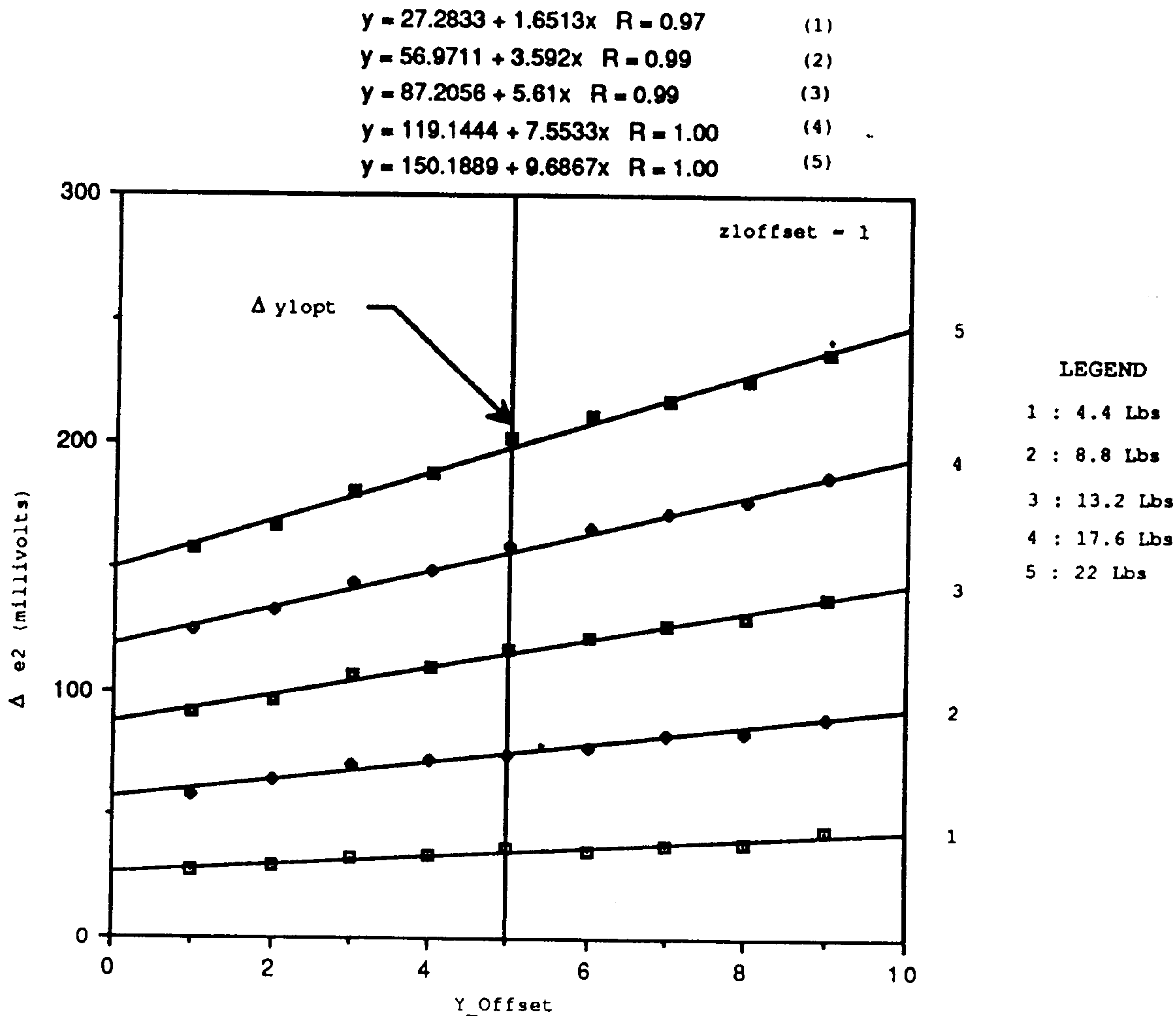

FIG. 20 Sensor Response Δe_2 V/S Δy_1 (Δz_1 = 1)

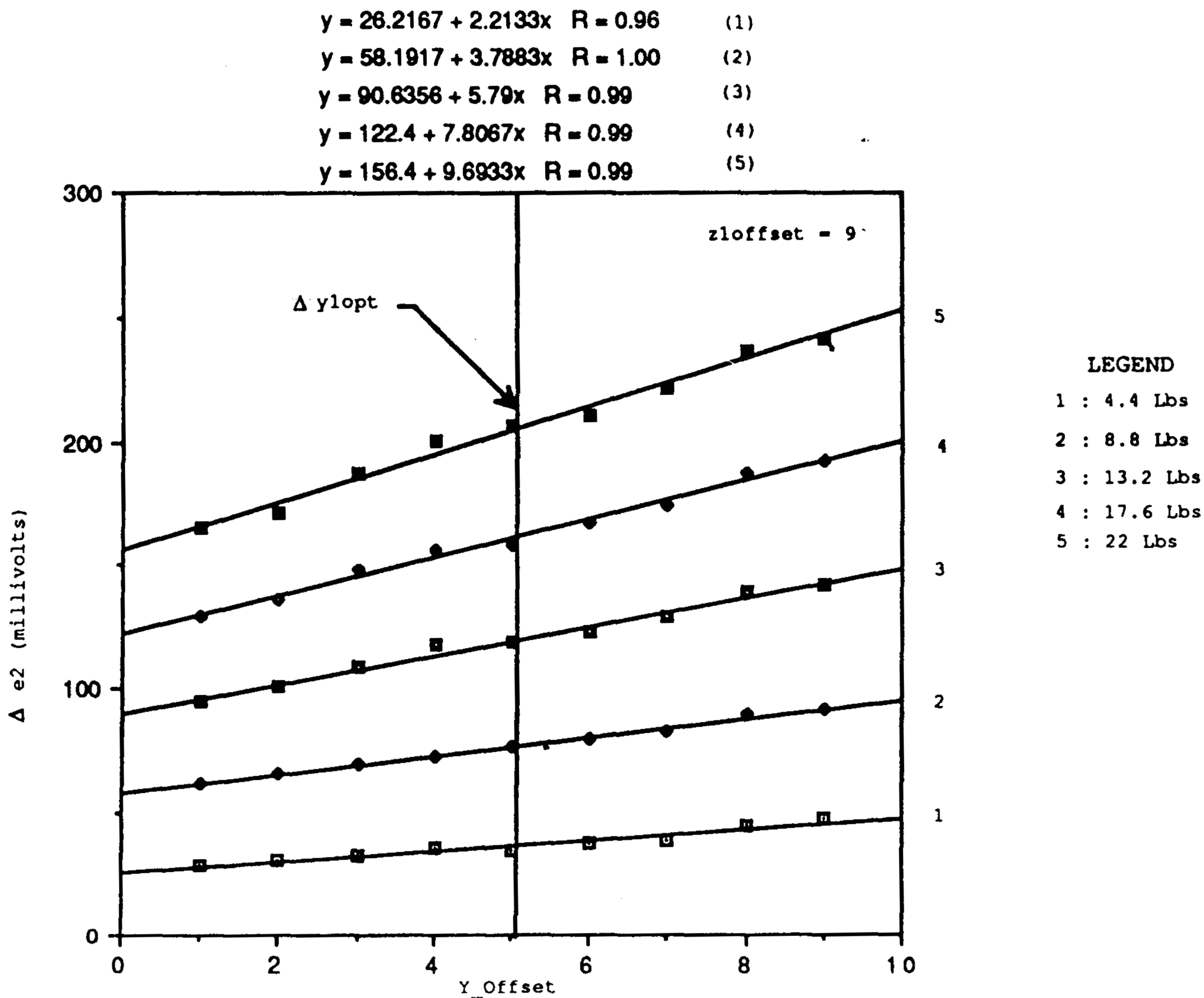

FIG. 21 Sensor Response Δe_2 V/S Δy_1 (Δz_1 = 9)

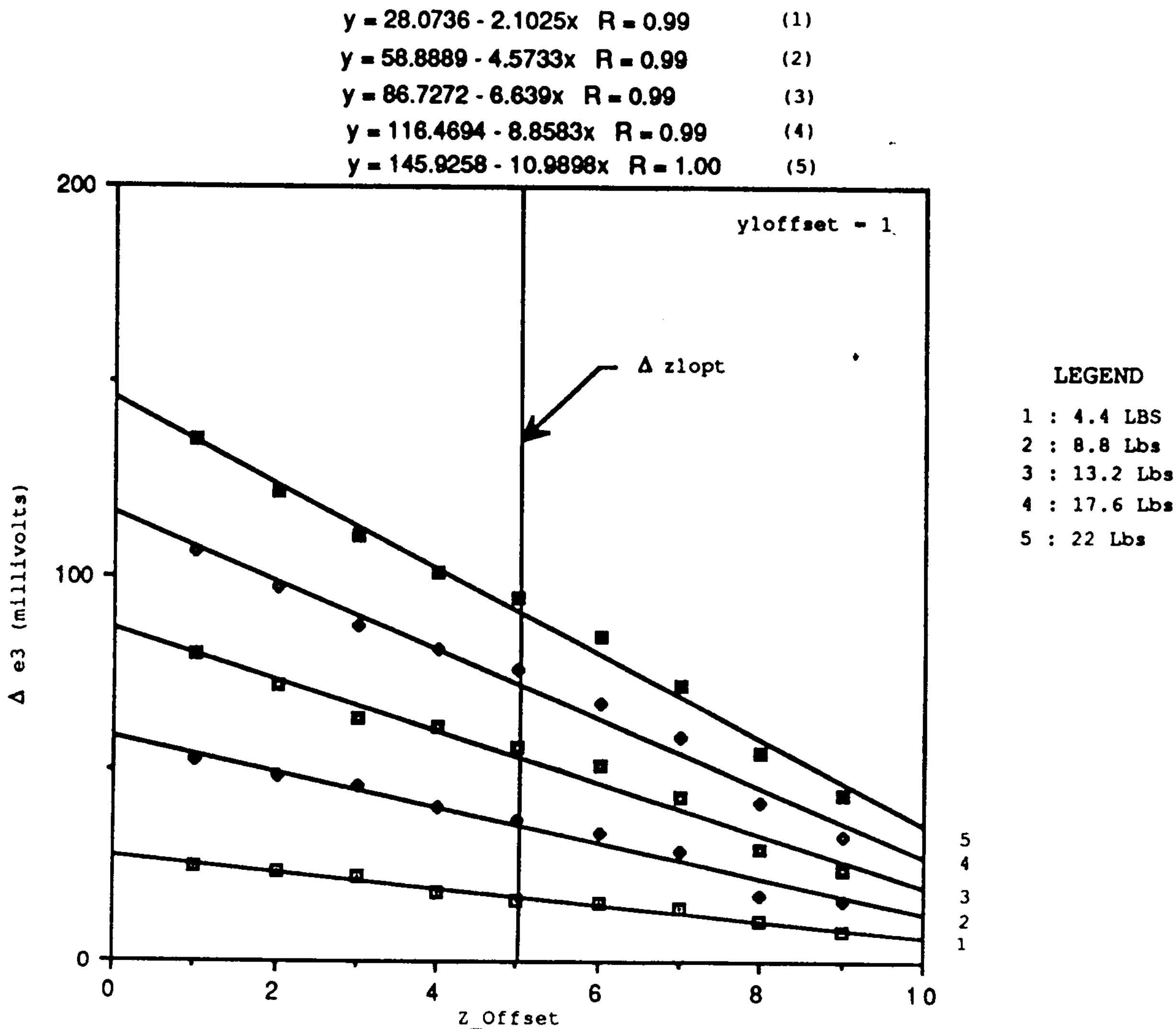

FIG. 22 Sensor Response Δe_3 V/S Δz_1 ($\Delta y_1 = 1$)

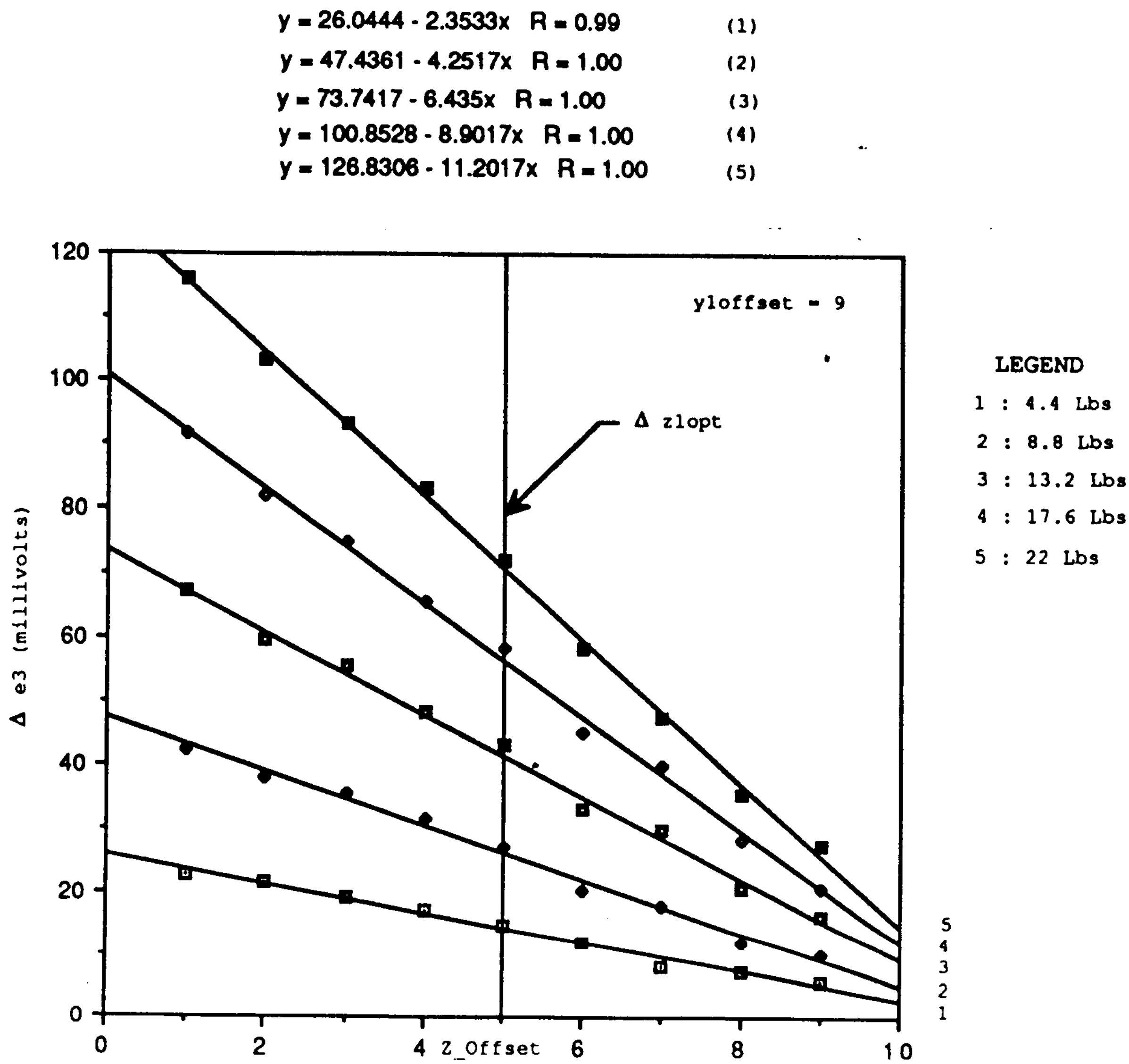

FIG. 23 Sensor Response Δe_3 V/S Δz_1 ($\Delta y_1 = 9$)

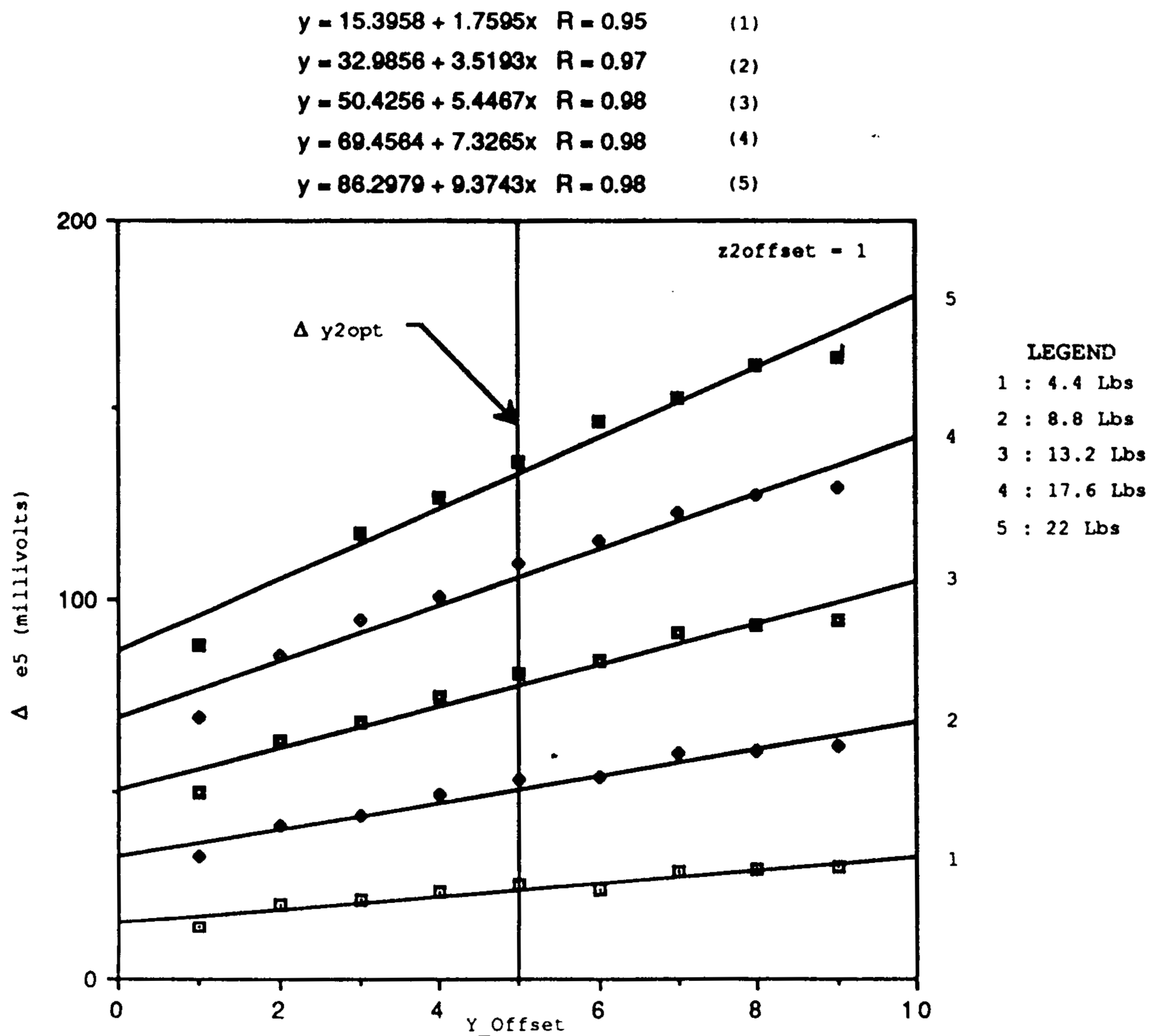

FIG. 24 Sensor Response Δe_5 V/S Δy_2 (Δz_2 = 1)

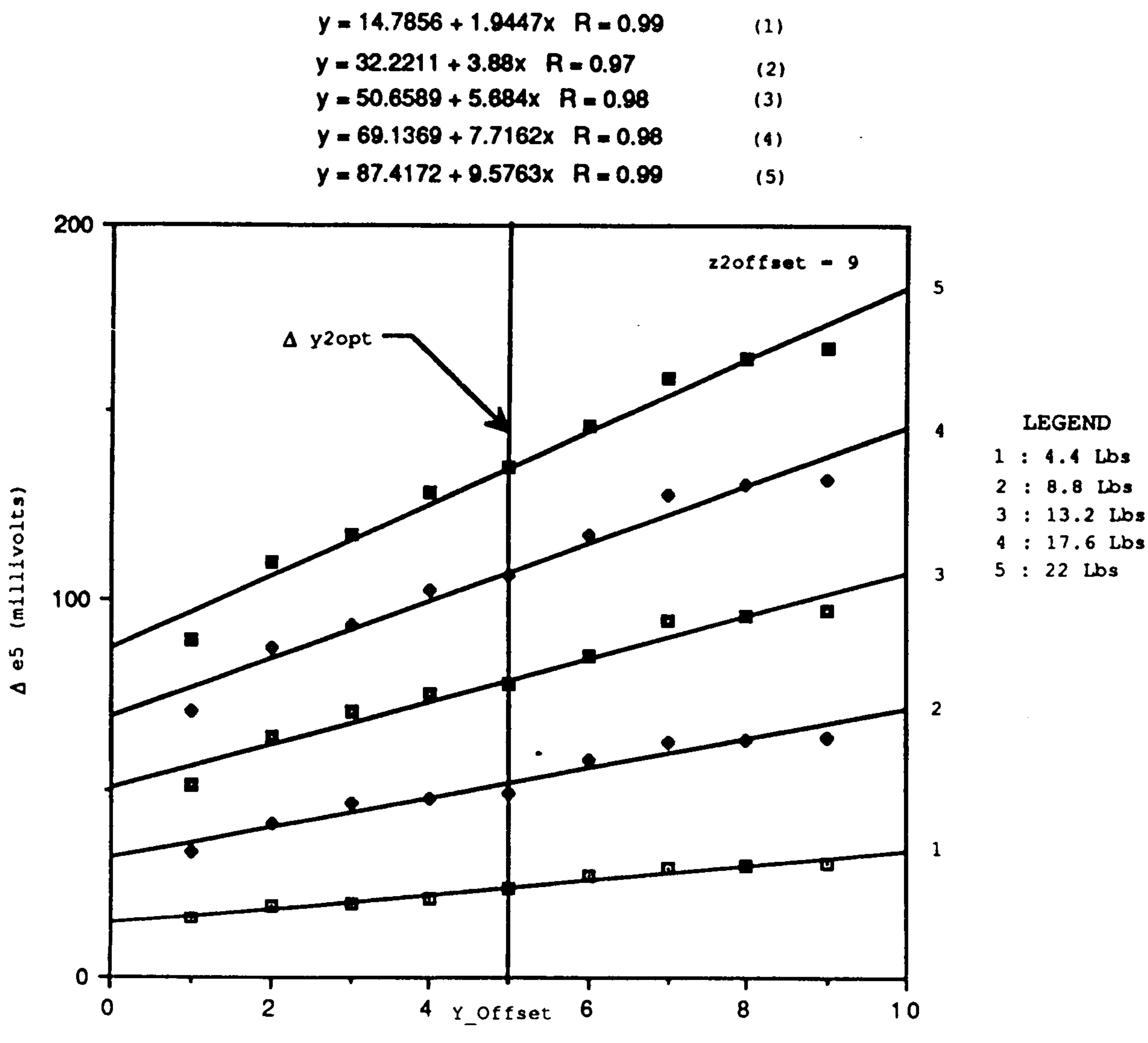

FIG. 25 Sensor Response Δe_5 V/S Δy_2 (Δz_2 = 9)

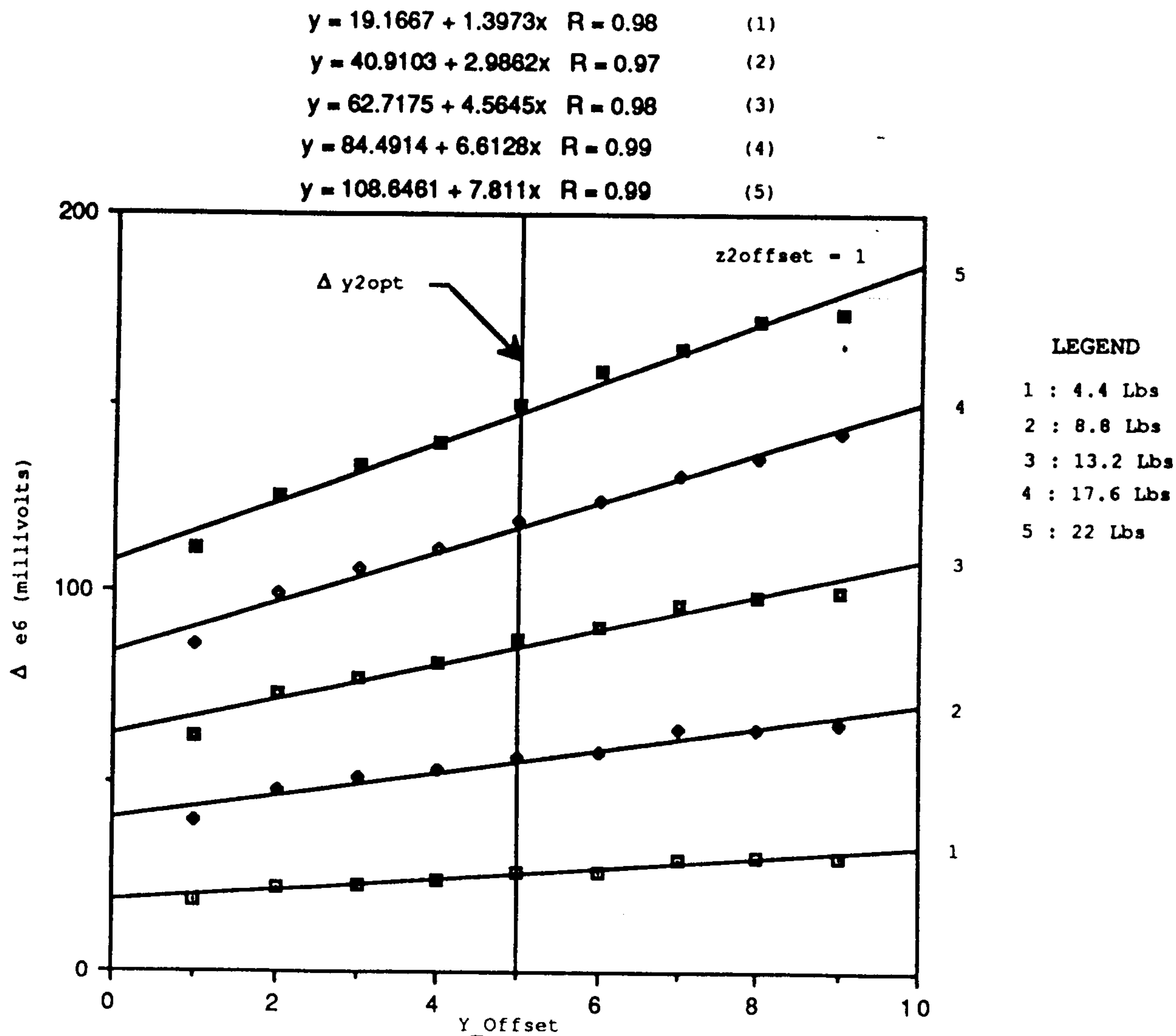

FIG. 26 Sensor Response Δe_6 V/S Δy_2 (Δz_2 = 1)

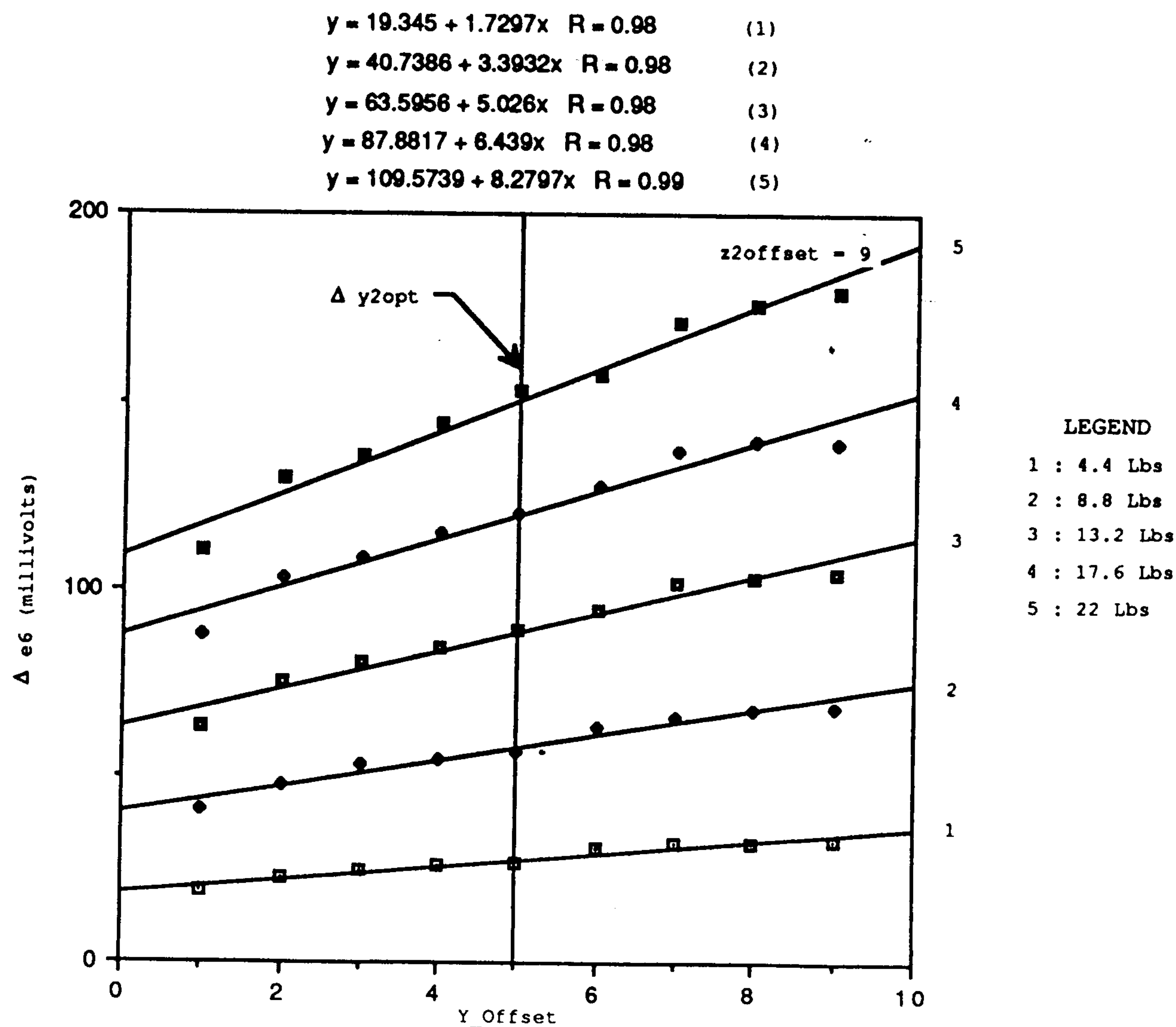

FIG. 27 Sensor Response Δe_6 V/S Δy_2 ($\Delta z_2 = 9$)

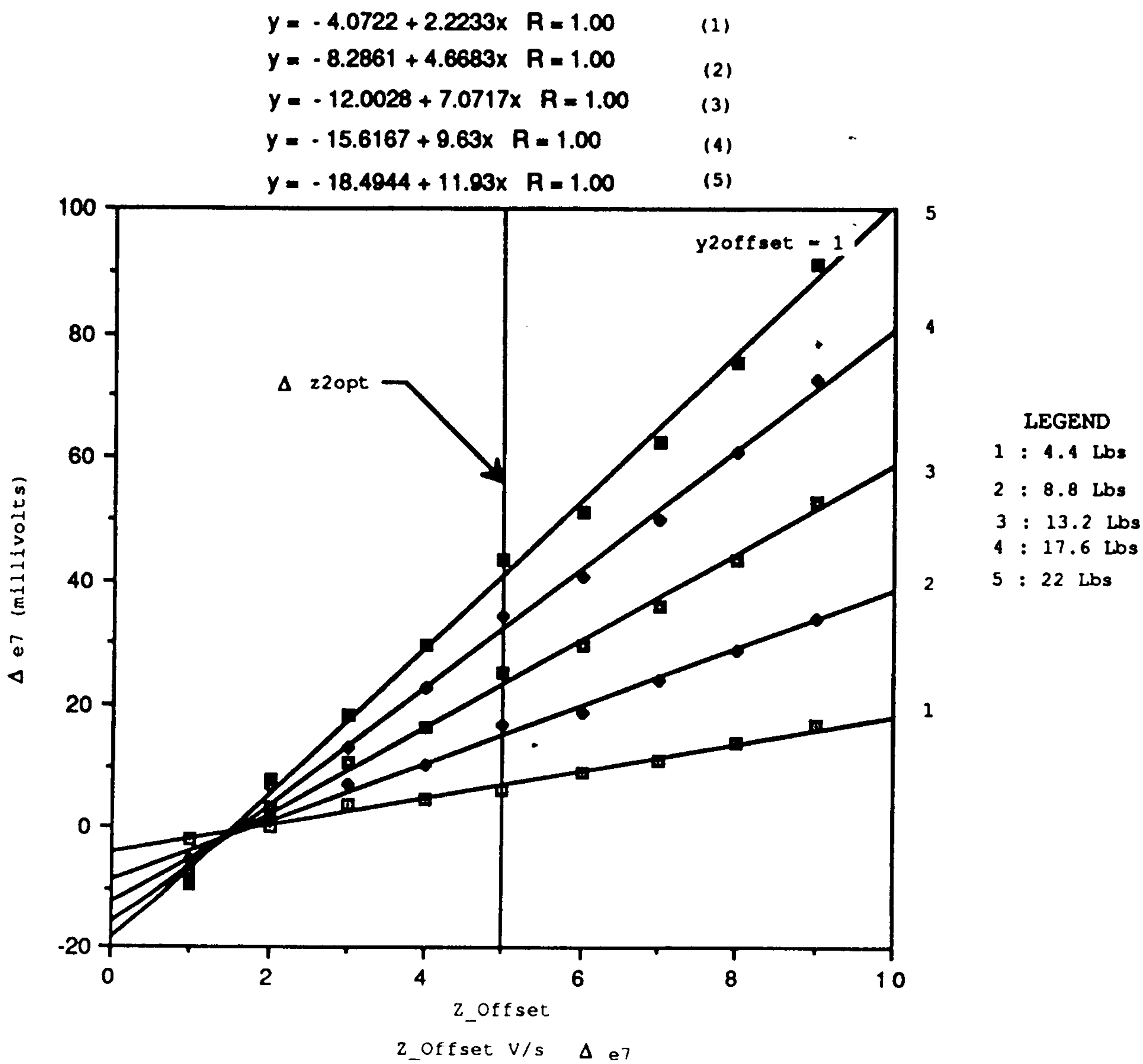

FIG. 28 Sensor Response Δe_7 V/S Δz_2 (Δy_2 = 1)

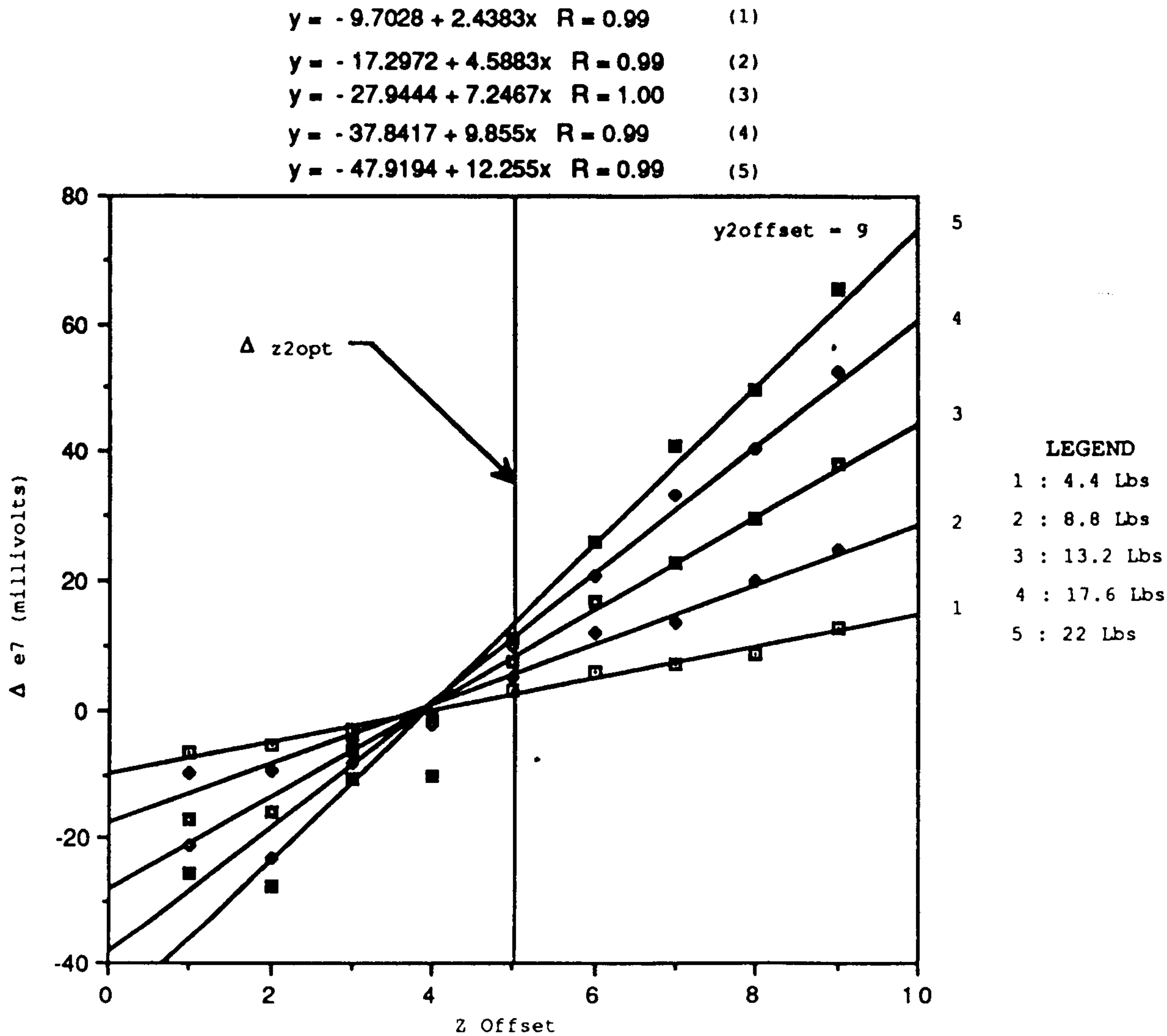

FIG. 29 Sensor Response Δe_7 V/S Δz_2 (Δy_2 = 9)

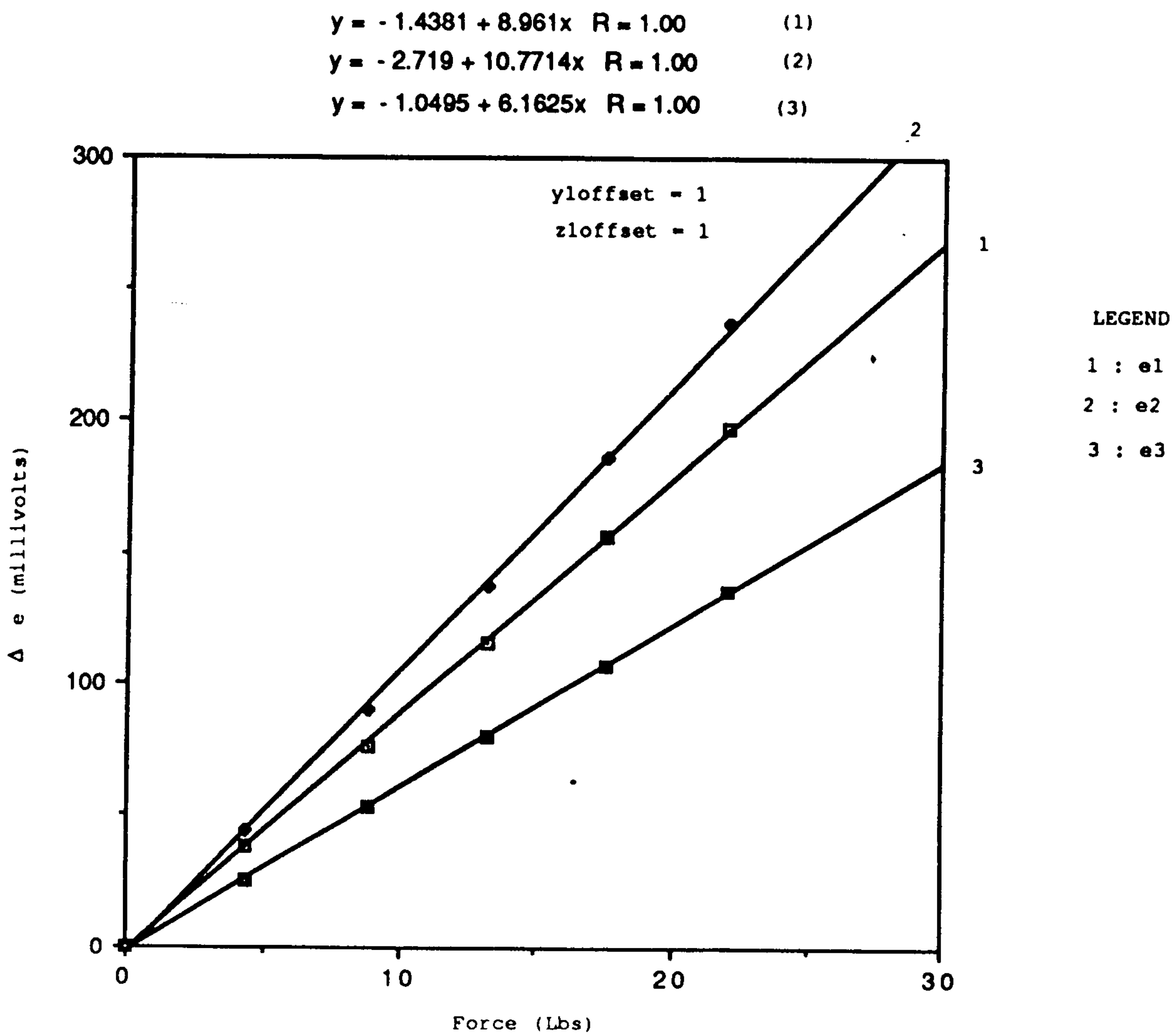

FIG. 30 Sensor Response V/S Applied Force (Finger 1)

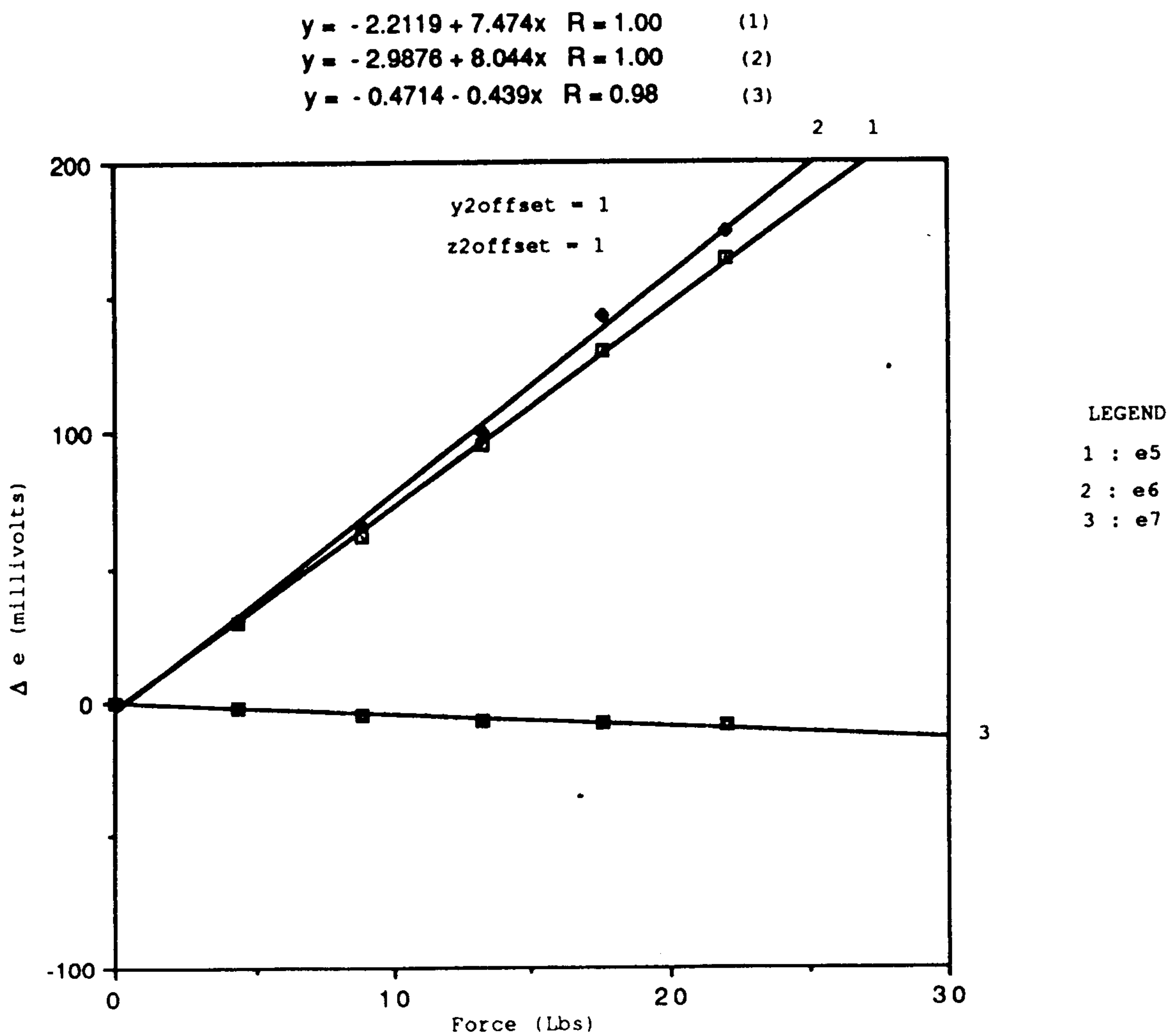

FIG. 31 Sensor Response V/S Applied Force (Finger 2)

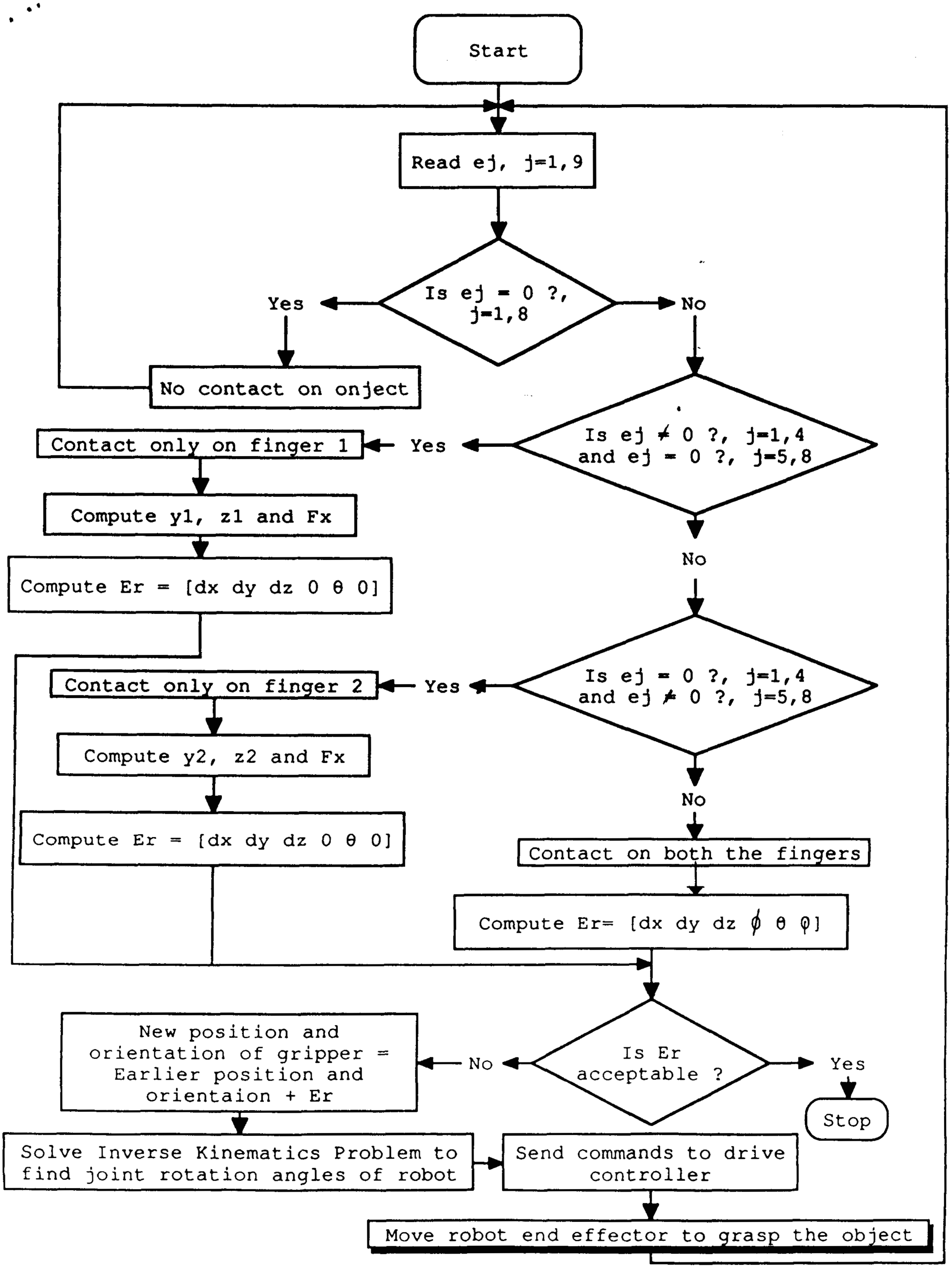

FIG. 32 Flow Chart For Control Algorithm